The final authenticated version is available online at: https://doi.org/10.1161/CIRCULATIONAHA.122.060860

SUPPLEMENTAL MATERIAL

NLRP3 Inflammasome Activation Through Heart-Brain Interaction Initiates Cardiac Inflammation and Hypertrophy During Pressure Overload

Yasutomi Higashikuni, MD, PhD*; Wenhao Liu, MD; Genri Numata, MD, PhD; Kimie Tanaka, MD, PhD; Daiju Fukuda, MD, PhD; Yu Tanaka, MD, PhD; Yoichiro Hirata, MD, PhD; Teruhiko Imamura, MD, PhD; Eiki Takimoto, MD, PhD; Issei Komuro, MD, PhD; Masataka Sata, MD, PhD*

* Co-corresponding authors.

EXPANDED METHODS

Animal Study

All experiments were approved by the University of Tokyo Ethics Committee for Animal Experiments, and strictly adhered to the guidelines for animal experiments of the University of Tokyo. Eight- to 12-week-old male mice were used. Wild-type C57BL/6 mice were purchased from Takasugi Experimental Animal Supply (Saitama, Japan). *Nlrp3*$^{-/-}$ mice were provided by the laboratory of Dr. Jurg Tschopp (The University of Lausanne, Switzerland).[18] *P2rx7*$^{-/-}$ and *Slc17a9*$^{flox/flox}$ mice were purchased from the Jackson Laboratory (Maine, USA). DBH-*Cre* mice were provided by RIKEN BRC through the National Bio-Resource Project of MEXT, Japan (Tsukuba, Japan).[19]

Pressure overload was induced by transverse aortic constriction (TAC) as described previously.[4] Briefly, mice were anesthetized by intra-peritoneal injection of sodium pentobarbital (50 mg/kg body weight). A 24-gauge polyethylene tube was inserted into the trachea and mechanical ventilation was provided by a rodent ventilator. The chest was opened through a second left intercostal incision and the transverse aortic arch was exposed. The transverse aorta was banded between the brachiocephalic and left common carotid arteries to the diameter of a 25-gauge needle using a 7-0 nylon suture. Sham animals were prepared identically without undergoing banding of the transverse aorta.

Apyrase (4 units, Sigma, St. Louis, Missouri, USA), lipopolysaccharide (2mg/kg; 14945-81; InvivoGen, San Diego, California, USA), 2'(3')-O-(4-benzoylbenzoyl)-ATP (5mg/kg; B6396; Sigma), MCC950 (10mg/kg; S7809; Selleck Chemicals, Houston, Texas, USA), and clonidine (10μg/kg, Sigma) were injected intraperitoneally daily. Anti-IL-1 antibody (100 μg per mouse; AB-401-NA; R&D Systems, Minneapolis, Minnesota, USA) or control anti-gout IgG antibody

(100μg per mouse; AB-108-C; R&D Systems) was injected intravenously. Pseudoephedrine (20mg/kg/day, Ieda Chemicals Co., Ltd., Tokyo, Japan) and bisoprolol hemifumarate (5mg/kg/day, Tokyo Chemical Industry Co., Ltd., Tokyo, Japan) were orally administered to mice by gavage daily. Isoproterenol (Sigma-Aldrich, St. Louis, Missouri, USA) was administered to mice via an osmotic minipump (30mg/kg/day, ALZET mini-osmotic pump, DURECT Corporation, Cupertino, California, USA). Left stellate ganglionectomy was performed just before TAC or sham operation.[20] To ablate primary afferent neurons, subepicardial injection of capsaicin (50mg/ml, Sigma) dissolved in olive oil (Wako, Osaka, Japan) was performed at 2 weeks before induction of TAC.[21]

Mice were randomly allocated to groups, and littermates were split across groups. Investigators were not fully blinded to mouse genotypes and treatment groups during experiments due to logistical issues in animal care.

Human Samples

The use of previously obtained human heart biopsy samples from heart failure patients for daily practice was approved by the Institutional Review Board of the University of Tokyo Hospital, and consent was obtained from all subjects. These samples were fixed in 10% formalin and embedded in paraffin.

Echocardiographic and Hemodynamic Measurements

Transthoracic echocardiographic study was performed under anesthesia with sodium pentobarbital with a dynamically focused 15MHz linear-array transducer (EnVisor M2540A; Philips Medical System, Best, The Netherlands) with a depth setting of 1.5 cm or the Vevo 3100 Imaging System

(FUJIFILM VisualSonics Co., Bothell, WA, USA). M-mode tracings were recorded from the short axis view at the papillary muscle level of the left ventricle (LV). For hemodynamic measurement, the right carotid artery was cannulated by the micro pressure transducers with an outer diameter of 0.42mm (Samba 201 and Samba Preclin 420 LP; Samba Sensors AB, Vastra Frolunda, Sweden), which was then advanced into the LV.[4] Pressure signals were recorded using a MacLab data acquisition system (Model 400 with chart v4.2 software; AD Instruments, Colorado Springs, CO, USA) with a sampling rate of 5000Hz. Heart rate was kept at approximately 250-350 beats per minute to minimize data deviation. Blood pressure of conscious mice was measured with the tail-cuff method (Softron BP-98A; Softron Co., Tokyo, Japan).

Bone Marrow Transplantation Experiment

A bone marrow transplantation experiment was performed as described previously.[4] Briefly, 8-week-old male wild-type mice were subjected to irradiation with a total dose of 9 Gy followed by bone marrow reconstitution by tail vein injection of 1.0×10^7 bone marrow cells isolated from donor femurs and tibias of wild-type or *Nlrp3*$^{-/-}$ mice. Four weeks after bone marrow transplantation, mice were subjected to TAC or sham operation. With this protocol, peripheral blood cells of recipient mice consist of more than 95% donor cells.[4]

***In Vivo* ATP Measurement Using Enzyme-Based Biosensors**

An ATP biosensor system was purchased from Sarissa Biomedical (West Midlands, UK). The principal design and operation of the enzyme-based biosensors used in this paper have been described in detail elsewhere.[28] Mice were anesthetized and intubated for mechanical ventilation as described above. The chest was opened through a fourth left intercostal incision. Just before

ATP measurement, calibration was performed using ATP solution (Figure VIA in the Data Supplement). The reference electrode was inserted into the LV apical wall through a small incision made with a needle, then the ATP biosensor was inserted into the LV anterior wall (Figure 4A). Electric current between the reference electrode and the ATP biosensor was measured through a potentiostat (8100-K4; Pinnacle Technology, Lawrence, Kansas, USA) and transformed into ATP level based on the calibration curve. Insertion of the reference electrode and the ATP biosensor causes tissue injury, which leads to massive release of intracellular ATP from damaged cells into the extracellular space. To eliminate the influence of tissue injury, ATP level in the stable phase, in which the tendency of detected electric currents does not change, was measured as extracellular ATP concentration. Extracellular ATP level was calculated by averaging ATP levels at 60 time points (i.e. 60 seconds) in the stable phase. SIRENIA acquisition software (Pinnacle Technology) was used for data collection and analysis.

In Vivo ATP Measurement Using Recombinant Plasma Membrane-Targeted Luciferase

An engineered firefly luciferase, called pmeLUC, that localizes to the outer aspect of the plasma membrane with the catalytic site facing the extracellular environment,[29] was cloned into the adeno-associated virus 9 (AAV9) vector in the downstream of the chicken cardiac troponin T promoter. AAV9 was packaged by VectorBuilder (Chicago, IL, USA) and frozen at -80°C until use. AAV9 (3.2×10^{11} genome copies per mouse) was retro-orbitally injected into mice on the next day after TAC or sham operation. At day 14 after TAC, luciferin-containing PBS (150mg/kg, ab143655; abcam, Cambridge, UK) was injected intraperitoneally into mice, and luminescent signals were detected under isoflurane anesthesia by the IVIS luminometer (IVIS Spectrum; Xenogen, Alameda,

CA, USA) at 10 minutes after the injection. The average of luminescent signals within region of interest (i.e. the heart) was calculated for comparison.

Ex Vivo Isolated Heart Perfusion

Isolated murine hearts were perfused with warmed Tyrode's solution (T2145; Sigma-Aldrich) at 37°C using the Langendorff system.[37] Pressure overload of approximately 40 mmHg was applied on murine hearts by increasing perfusion pressure. LV pressure was measured and recorded using a mouse pressure-volume catheter (PVR-1035; Millar Instruments Inc., Houston, Texas, USA) and the MPVS Ultra Foundation System (ADInstruments, New South Wales, Australia) with LabChart 7 software (ADInstruments). Heart tissues after 60 minutes of perfusion were used for analysis.

Histological Analysis

Hearts were weighed and fixed in methanol. Samples were embedded in paraffin and sectioned at 5-μm thickness. Specimens were stained with hematoxylin and eosin (H&E) or sirius red dye as described previously.[4] Myocyte cross-sectional area (CSA) and collagen volume fraction (CVF) were determined by quantitative morphometric analysis of specimens with H&E and sirius red staining, respectively. Twenty cardiomyocytes per slide were measured for myocyte CSA calculation. Five random fields were examined for CVF analysis (magnification, ×200). ImageJ 1.52a (National Institutes of Health, Bethesda, Maryland, USA) was used for data analysis.

Immunohistochemical staining was performed with anti-NLRP3 antibody (1:50 for human samples; 1:200 for mouse samples; MAB7578, lot CGSM0114021; R&D Systems), anti-Mac-3 antibody (1:500; M3/84; 550292, lot 66716; BD Pharmingen, San Diego, California, USA), anti-CD31 antibody (1:200; MEC13.3; 550274, lot 58170; BD Pharmingen), anti-neurofilament

antibody (1:2000; AB5539, lot NG1928749; Millipore, Burlington, MA, USA), anti-tyrosine hydroxylase (TH) antibody (1:500; AB152, lot 2328305; Millipore), and anti-calcitonin gene-related peptide (CGRP) antibody (1:1000; PC205L, lot D00149648; Calbiochem, San Diego, CA, USA). Biotinylated anti-rat IgG antibody (1:500; BA-4001, lot WO918; Vector Laboratories, Youngstown, Ohio, USA), anti-chicken IgG antibody (1:2000; 603-4602, lot 20680; Rockland Immunochemicals, Inc., Pottstown, PA, USA), or anti-rabbit IgG antibody (1:1000; E0432, lot 20027287; Dako, Santa Clara, CA, USA) was used as a secondary antibody. Antibody distribution was visualized by the avidin-biotin complex technique with Vector Red substrate (Vector Laboratories). Macrophage density was assessed in specimens with anti-Mac-3 antibody, and five random fields were examined (magnification, ×400). Density was expressed as the number/square millimeter. Quantitative assessment of the number of vessels per cardiomyocyte was performed in specimens with anti-CD31 staining. The number of vessels per cardiomyocyte was counted in 50 cardiomyocytes. Total areas of epicardial TH-positive or CGRP-positive nerve fibers were measured using ImageJ 1.52a (National Institutes of Health). Histological images were obtained using ACT-2U ver. 1.61 (Nikon, Tokyo, Japan) or Motic Image Plus 2.3S (Motic, Hong Kong) software.

RNA Extraction and RT-PCR Analysis

Total RNA was isolated from myocardial tissues with TRIzol Reagent (Invitrogen Corp., Carlsbad, California, USA) and from cultured cells and stellate ganglions with a Total RNA Isolation Mini Kit (Agilent Technologies, Santa Clara, California, USA). Reverse transcription was performed with 1 μg total RNA, random hexamer primers and MMLV reverse transcriptase (ReverTraAce-α; TOYOBO, Osaka, Japan) for myocardial tissues and cultured cells. For stellate ganglions,

amplified cDNA was prepared with an Ovation PicoSL WTA System V2 (NuGEN Technologies, San Carlos, California, USA). For quantitative assessment of gene expression levels, quantitative real-time PCR analysis was performed. Specific mRNAs were quantified with SYBR Green real-time PCR Master Mix (TOYOBO) in a StepOnePlus™ Real-Time PCR System (Applied Biosystems, Foster City, California, USA) under standard manufacturer's conditions. Data are expressed in arbitrary units normalized by correction for the signal obtained in the same cDNA preparation for *Gapdh* mRNA. The primers for real-time PCR are shown in Table S1.

Immunoblotting

Proteins were extracted from myocardial tissues homogenized in RIPA Lysis and Extraction Buffer (G-Biosciences, St. Louis, Missouri, USA) with a protease inhibitor cocktail (Sigma-Aldrich) and a phosphatase inhibitor cocktail (Wako). Protein concentration was measured using Pierce BCA Protein Assay Reagent (Thermo Fisher Scientific, Waltham, Massachusetts, USA). Protein samples (20-50 μg) were separated by SDS-PAGE and transferred to a polyvinylidene fluoride membrane (Hybond-P; GE Healthcare, Little Chalfont, UK). The membrane was incubated with anti-NLRP3 antibody (1:1000; AG-20B-0014, lot A24971303; Adipogen, San Diego, California, USA), anti-TXNIP antibody (1:1000; NBP1-54578, lot 036; Novus Biologicals, Centennial, Colorado, USA), anti-caspase-1 antibody (1:200; sc-1218, lot K0812; Santa Cruz Biotechnology, Santa Cruz, California, USA), anti-ASC antibody (1:1000; AG-25B-0006, lot A25061305; Adipogen), anti-caspase-1 antibody (1:250; AG-20B-0042, lot A40231903; Adipogen), anti-interleukin (IL)-1β antibody (1:500; AB-401-NA, lot BO0710091; R&D Systems), anti-c-Myc antibody (1:200; sc-40, lot F2921; Santa Cruz Biotechnology), anti-glyceradldehyde-3-phosphate dehydrogenase antibody (1:1000; sc-32233, lot I2821; Santa Cruz

Biotechnology), or anti-β-actin antibody (1:5000; AC-15; A5441, lot 126K4755; Sigma-Aldrich), or anti-heat shock cognate protein 70 antibody (1:1000; sc-7298, lot K0921; Santa Cruz Biotechnology), followed by incubation with horseradish peroxidase-conjugated anti-goat IgG (1:20000; sc-2020, lot J298; Santa Cruz Biotechnology), anti-rabbit IgG (1:2500; HAF008, lot FIN1820071; R&D Systems), or anti-mouse IgG (1:5000; sc-2005, lot K1710; Santa Cruz Biotechnology) secondary antibody. An enhanced chemiluminescence system (ECL Plus or ECL Prime; GE Healthcare) was used for detection. Immunoblot images were obtained using LAS-3000Uvmini (Fuji Film, Tokyo, Japan) or LuminoGraph I (ATTO Corporation, Tokyo, Japan). Since the amount of cleaved caspase-1 in the heart was very small compared with that of procaspase-1, even in TAC-operated mice, possibly due to heterogeneous activation of caspase-1 in pressure-overloaded hearts, gray level correction was performed on output images for anti-caspase-1 antibody.

Measurement of Caspase-1 Activity in Murine Heart

For assessment of caspase-1 activity in murine hearts, the Caspase-Glo 1 Inflammasome Assay (Promega, Madison, Wisconsin, USA) was performed. Briefly, protein samples isolated from murine hearts were incubated with a luminogenic caspase-1 substrate, a recombinant luciferase and a proteasome inhibitor. Luminescence was measured by using a plate-reading luminometer (GloMax-Multi Detection System; Promega). A mouse recombinant active caspase-1 (1181-100, lot 6C11L11810; BioVision, Milpitas, CA, USA) was used for a calibration curve. To examine the specificity for the detection of caspase-1 activity, samples were tested with a selective caspase-1 inhibitor.

Measurement of IL-1β in Murine Heart

For assessment of IL-1β level in murine hearts, a mouse ELISA kit (MLB00C; R&D Systems) was used according to the manufacturer's recommendations. Values were normalized to total protein level. Protein concentration was measured using Pierce BCA Protein Assay Reagent (Thermo Fisher Scientific). A plate reader (POWERSCAN HT; DS pharma biomedical, Osaka, Japan) with Gen5 software (Biotek, Winooski, Vermont, USA) was used for data collection.

Measurement of Norepinephrine Concentration in Murine Heart and Plasma

For assessment of norepinephrine concentration in murine hearts and plasma, a norepinephrine ELISA kit (KA1891; Abnova, Taipei City, Taiwan) was used according to the manufacturer's recommendations. For homogenized heart tissue samples, values were normalized to tissue weight. A plate reader (iMark; Bio-Rad Laboratories, Hercules, CA, USA) was used for data collection.

Quantification of Mitochondrial DNA Content and Oxidative Damage

For assessment of mitochondrial DNA (mtDNA) content in murine hearts, mtDNA to nuclear DNA (nDNA) ratios were measured.[23] DNA was extracted from myocardial tissues using NucleoSpin TriPrep (740966; MACHEREY-NAGEL, Dueren, Germany) and subjected to quantitative real-time PCR with specific primer sets for Cytochrome b (mtDNA) and β-actin (nDNA). The primers were as the follows: Cytochrome b, 5'-GCTTTCCACTTCATCTTACCATTT-3' and 5'-TGTTGGGTTGTTTGATCCTG-3'; β-actin, 5'-GGAAAAGAGCCTCAGGGCAT-3' and 5'-GAAGAGCTATGAGCTGCCTGA-3'.

For assessment of mtDNA oxidative damage in murine hearts, 8-hydroxy-2'-deoxyguanine (8-OHdG) level in mtDNA was measured. MtDNA was isolated from murine hearts by using

mtDNA Extractor CT kit (291-55301; Fuji Film). OxiSelect Oxidative DNA Damage ELISA kit (STA-320; Cell Biolabs, San Diego, California, USA) was used for detection of 8-OHdG in mtDNA. Values were normalized to mtDNA level. A plate reader (ARVO X3; PerkinElmer, Waltham, Massachusetts, USA) was used for data collection.

Cell Cultures

Human microvascular endothelial cells from the heart (HMVEC-C) were purchased from Lonza (Basel, Switzerland). HMVEC-C were cultured using an EGM-2-MV BulletKit (Lonza). Cardiomyocytes and fibroblasts were prepared from neonatal rats and cultured as described previously.[4] Neonatal Wistar rats were purchased from Takasugi Experimental Animal Supply (Saitama, Japan). Neonatal ventricles from 1-day-old Wistar rats were separated and minced in ice-cold balanced salt solution. For isolation of cardiac cells, the tissues were incubated in a balanced salt solution containing 0.2% collagenase type 2 (Worthington Biochemical, Lakewood, New Jersey, USA) for 7 minutes at 37°C with agitation. The digestion buffer was replaced seven times. The dispersed cells were incubated in 100-mm culture dishes for 90 minutes to remove non-myocytes. The unattached viable cells, which were rich in cardiomyocytes, were cultured on collagen type I-coated dishes at 37°C in DMEM supplemented with 10% fetal bovine serum (FBS). Non-myocyte cells that attached to the dishes were cultured in DMEM supplemented with 10% FBS and allowed to grow to confluence. Then, they were trypsinized and passaged. Cell cultures yielded by this procedure were used as cardiac fibroblasts.[4]

***In Vitro* Experiments**

Nlrp3 knockdown was performed using NLRP3 siRNA (Sigma-Aldrich) and the N-TER Nanoparticle siRNA Transfection System (Sigma-Aldrich) according to the manufacturer's protocol. Scrambled siRNA (Sigma-Aldrich) was transfected as a control experiment. For inhibition of the P2X7 receptor, o-ATP (100μM, Sigma), a P2X7 receptor antagonist, was used. Anti-IL-1β antibody and control IgG (5μg/ml for cardiomyocytes and cardiac fibroblasts; 2.5μg/ml for HMVEC-C; R&D Systems) was used for IL-1β neutralization. Cardiomyocytes, cardiac fibroblasts, and HMVEC-C were stimulated with ATP (100μM for cardiomyocytes, 1μM for fibroblasts and HMVEC-C; Sigma), norepinephrine (2μM, Sigma), or a specific synthetic ligand for TLR2, Pam3CSK4 (300ng/ml, InvivoGen).[4]

Cardiomyocyte hypertrophy was assessed by cardiomyocyte size after 48-hour stimulation. Cardiomyocyte size was determined by measuring the cell surface area of sarcomeric α-actinin-positive cells identified by immunocytochemical staining.[4] Briefly, cardiomyocytes were fixed in 2% paraformaldehyde and permeabilized for 10 minutes with 0.2% Triton-X (Sigma-Aldrich) in PBS. After blocking with PBS containing 2% FBS for 10 minutes, they were then incubated with anti-sarcomeric α-actinin antibodies (1:500; A7811, lot 072K4862; Sigma-Aldrich), followed by treatment with Alexa Fluor 488-conjugated secondary antibodies (1:500; A21202, lot 898250; Molecular Probes, Eugene, Oregon, USA). Images were obtained using InStudio software (Pixera, Osaka, Japan). ImageJ 1.52a (National Institutes of Health) was used for data analysis.

Proliferation of cardiac fibroblasts and vascular endothelial cells was assessed after 24-hour stimulation with ATP, norepinephrine, or Pam3CSK4 by MTS (dimethylthiazol-carboxymethoxyphenyl-sulfophenyl-tetrazolium) assay (CellTiter 96 AQueous One Solution Assay; Promega). The percentage of the absorbance of a well with cells under control treatment was calculated.[4] Data are expressed as a fold-change relative to the control group. A plate reader

(POWERSCAN HT; DS pharma biomedical) with Gen5 software (Biotek) was used for data collection.

Statistical Analyses

Statistical analyses were performed with EZR (Saitama Medical Center, Jichi Medical University, Saitama, Japan), which is a graphical user interface for R (The R Foundation for Statistical Computing, Vienna, Austria).[22] More precisely, it is a modified version of R commander, designed to add statistical functions frequently used in biostatistics.

Differences in means between two groups were analyzed by unpaired two-tailed t-test. More than two groups were compared using one-way analysis of variance (ANOVA) followed by Holm test or Dunnett's test for multiple comparison. The Kaplan-Meier method with log-rank test was used for survival analysis. Values of $P<0.05$ were considered statistically significant.

EXPANDED DISCUSSION

In this study, we demonstrated that neural signals control cardiac inflammation and hypertrophy through NLRP3 inflammasome activation during pressure overload (Figure 8). Mechanistically, ATP released from SEN terminals activates the NLRP3 inflammasome in cardiac non-immune cells through stimulation of the P2X7 receptor, which, together with TLR signaling, leads to IL-1β production to induce cardiac adaptive hypertrophy. Pressure overload is sensed by cardiac afferent nerves to activate SENs for ATP release. The CNS might be involved in this mechanism to modulate SNS activity.

IL-1β is a key proinflammatory cytokine that contributes to the pathophysiology of hypertrophic heart disease.[4,11] Active IL-1β production is tightly controlled in a two-step process.[10] The first step upregulates the inactive precursor, pro-IL-1β, by promoting the transcription of IL-1β gene. The second step processes pro-IL-1β into active IL-1β by activating caspase-1. In the heart, the first step is activated by local proinflammatory mechanisms, in which DAMPs from damaged cardiac cells stimulate innate immune receptors for NF-κB activation in an autocrine and paracrine manner.[4,5] Our data show that the second step is regulated by the nervous system and the brain through NLRP3 inflammasome activation. Thus, both local mechanisms and organ communications are necessary for proinflammatory process in the heart. In this study, we found that NLRP3, ASC, and procaspase-1 proteins in the heart are expressed at detectable levels at baseline, which might explain why caspase-1 was activated by treatment with BzATP or pseudoephedrine alone without priming signals for upregulation of inflammasome components.[42] However, BzATP or pseudoephedrine treatment with our dose did not induce IL-1β production or cardiac hypertrophy, suggesting a significant impact of priming signals on pathological cardiac remodeling during pressure overload. Neural regulation of NLRP3 inflammasome activity might play an important role in preventing uncontrolled inflammation and maintaining homeostasis of

the whole body. In addition, our proposed mechanism, in which the distribution of SEN terminals might affect proinflammatory responses in the organ, might explain the heterogeneity of cellular responses in the pressure-overloaded heart.[43]

In our study, genetic disruption of NLRP3 resulted in contractile dysfunction and hemodynamic maladaptation with high mortality after TAC, while it inhibited cardiac hypertrophy and progression of pathological cardiac remodeling during pressure overload. Pathological changes of cardiomyocytes were not observed in pressure-overloaded *Nlrp3*$^{-/-}$ hearts. This cardiac phenotype is similar to that of wild-type mice treated with anti-IL-1β antibodies in our previous study.[4] Recent animal experiments and clinical trials have demonstrated that cardiac hypertrophy is not universally required for functional adaptation to hemodynamic stress.[44] Further studies will be necessary to elucidate how IL-1β signaling contributes to hemodynamic adaptation to pressure overload, independent of hypertrophic change in cardiomyocytes. Inflammation is a double-edged sword that has both protective and harmful effects under various pathological conditions. For example, the Canakinumab Anti-inflammatory Thrombosis Outcome Study (CANTOS) trial demonstrated that anti-IL-1β antibody treatment led to a significantly lower rate of recurrent cardiovascular events, such as nonfatal myocardial infarction, nonfatal stroke, and cardiovascular death, in post-myocardial infarction patients,[39] while treatment with anti-IL-1β antibodies was reported to result in inhibition of fibrous cap formation and beneficial outward vessel remodeling for the maintenance of plaque stability and lumen diameter in a murine model of atherosclerosis.[40] Therapeutic strategies targeting inflammation might need fine-tuning of signaling pathways. Recently, NLRP3 inflammasome inhibitors have been suggested to be effective for the treatment of cardiovascular disease.[12,15,41,42] Our findings suggest that similarly to β-adrenergic receptor

blockers, careful titration of NLRP3 inflammasome inhibitors might be necessary for inhibition of pathological cardiac remodeling without hemodynamic maladaptation.

In this study, there are several findings that suggest an important role of an interaction between NLRP3 inflammasome-mediated inflammation and other signaling pathways in the pathophysiology of hypertensive heart disease. First, the ratios of NLRP3 and IL-1β mRNAs to ASC and procaspase-1 mRNAs in the pressure-overloaded heart were smaller than those in the LPS-treated heart. NF-κB signaling might be altered by other signaling pathways during pressure overload. Second, gene and protein expression levels of inflammasome components, especially procaspase-1 and IL-1β, were discrepant in the pressure-overloaded heart, which suggests an importance of RNA or post-translational modification. Third, while the combination of BzATP and LPS increased myocardial IL-1β level to a greater extent than pressure overload, the impact of the combination treatment on cardiomyocyte hypertrophy was smaller than that of pressure overload. This observation suggests that NLRP3 inflammasome-mediated inflammation might synergistically induce cardiomyocyte hypertrophy with other hypertrophic signaling pathways in the pressure-overloaded heart. Collectively, it would be important to elucidate how NLRP3 inflammasome-mediated inflammation and other signaling pathways modulate each other in cardiac cells in future studies.

The NLRP3 inflammasome components have been identified not only in immune cells, but also in non-immune cells, including cardiomyocytes, fibroblasts and vascular endothelial cells.[13,14] In myocardial infarction, the disease in which massive cell death occurs due to the loss of blood supply, danger signals from necrotic cardiac cells have been suggested to activate the NLRP3 inflammasome in alive cardiac cells for IL-1β production in an autocrine and paracrine manner, which promotes local inflammation and structural remodeling in the heart.[9,13,14] The NLRP3

inflammasome activation in bone marrow-derived immune cells further augments tissue injury.[9] In hypertensive heart disease, in which massive cell death does not occur, the role and underlying mechanisms of NLRP3 inflammasome activation in cardiac cells, however, remain unclear. Suetomi et al. reported that Ca^{2+}/calmodulin-dependent protein kinase IIδ (CaMKIIδ) is involved in NLRP3 inflammasome activation in cardiomyocytes at day 3 after TAC through ROS production.[15] They also found that cardiomyocyte-specific deletion of CaMKIIδ or pharmacological inhibition of the NLRP3 inflammasome with MCC950 mitigates cardiac inflammation, contractile dysfunction, and ventricular dilation and fibrosis in the chronic phase of pressure overload. Wang et al. showed that the NLRP3 inflammasome is activated in cardiac fibroblasts during pressure overload through both ROS-dependent and ROS-independent pathways.[17] They also demonstrated that an anti-fibrotic drug, pirfenidone, suppresses NLRP3 inflammasome activation and cardiac fibrosis in the pressure-overloaded heart. These reports suggest that NLRP3 inflammasome activation in cardiac cells might initiate cardiac inflammation and pathological cardiac remodeling during pressure overload, which is consistent with our study. In addition, ROS might be involved in NLRP3 inflammasome activation in response to pressure overload. In the present study, however, we found that TXNIP, which has been suggested to be the main actuator for NLRP3 inflammasome activation by ROS,[24] was not upregulated during pressure overload. This finding indicates that ROS might have indirect mechanisms, in addition to direct mechanisms, for NLRP3 inflammasome activation. Recently, cytosolic oxidized mtDNA has been suggested to activate the NLRP3 inflammasome in bone marrow-derived macrophages.[45] Since mtDNA oxidative damage was increased in the pressure-overloaded wild-type heart, this mechanism might contribute to NLRP3 inflammasome activation in cardiac cells. On the other hand, oxidized mtDNA was not increased in *Nlrp3*$^{-/-}$ hearts during pressure overload, suggesting

that hypertrophic or proinflammatory signals might be necessary for mitochondrial ROS production. Collectively, oxidized mtDNA might not be an initiator, but could be an accelerator, of NLRP3 inflammasome activation in the pressure-overloaded heart. It was reported that ROS activates primary afferent nerves.[46] Thus, ROS might play an important role in heart-brain interaction for NLRP3 inflammasome activation in the pressure-overloaded heart. In this study, how cardiac afferent nerves are activated in response to pressure overload remains unelucidated. Further studies are needed to clarify whether cardiac afferent nerves directly sense mechanical stress or chemical mediators released by cardiac cells in response to pressure overload.

Accumulating evidence has demonstrated a pivotal role of the SNS and its neurotransmitters in the regulation of inflammation.[47] For example, immune cells, such as macrophages and lymphocytes, respond to norepinephrine via adrenergic receptors and modulate inflammation in arthritis.[47] In addition, norepinephrine can induce cardiomyocyte hypertrophy and proliferation of fibroblasts and vascular endothelial cells by activating the adrenergic receptors.[48] The SNS is activated in pressure-overloaded mice and patients with heart failure, and is involved in cardiac remodeling.[31,49] Xiao et al. reported that proinflammatory cytokine expression and macrophage infiltration was suppressed in *Nlrp3*$^{-/-}$ hearts compare with *Nlrp3*$^{+/+}$ hearts at day 3 after a single injection of isoproterenol.[16] In our study, however, cardiac remodeling and the increase in the number of cardiac macrophages were similarly observed in *Nlrp3*$^{+/+}$ and *Nlrp3*$^{-/-}$ hearts after 14 days of continuous isoproterenol infusion. Furthermore, apyrase-treated mice or *Slc17a9*$^{-/-}$ mice, in which extracellular ATP was depleted without affecting myocardial norepinephrine levels, showed suppressed macrophage infiltration and cardiac hypertrophy during pressure overload. These findings suggest that ATP, rather than norepinephrine, might be the main neurotransmitter that initiates cardiac inflammation and hypertrophy, at least in the adaptive phase

of pressure overload, although β-adrenergic signals in the heart might have an interaction with the NLRP3 inflammasome and contribute to pathological cardiac remodeling in both NLRP3 inflammasome-dependent and -independent manners. Taken together with the data on bisoprolol-treated mice, lipophilic β-adrenergic receptor blockers, which are used as standard therapy for cardiac remodeling and heart failure,[36] might act on the brain, as well as on the heart, to inhibit SNS signals and cardiac inflammation with its ability to cross the blood-brain barrier. Further studies are needed to clarify the cross-talk between NLRP3 inflammasome activation and β-adrenergic signals in hypertensive heart disease.

The CNS has been implicated in the pathophysiology of heart disease.[37] It was reported that ROS and inflammatory cytokines are produced in the CNS during pressure overload, which activates the SNS and causes heart failure.[37] Okada et al. reported that the CNS senses ischemic insults in the heart via the cardiac afferent nerves, and secretes brain-derived neurotrophic factor, which protects the heart.[21] Fujiu et al. reported that cardiac resident macrophage activation is regulated by the heart-brain-kidney interaction through neural signals.[8] Our results suggest an important role of direct interaction between the heart and the CNS via neural signals in cardiac inflammation and remodeling. These mechanisms might link psychological distress to heart disease.[38]

In the present study, we demonstrated the contribution of input and output neural signals to NLRP3 inflammasome activation in the pressure-overloaded heart. However, the data processing mechanism in the complex nervous system remains unelucidated. TAC model is not a physiologically relevant disease model, and thus, activation patterns of the autonomic nervous system and the CNS in TAC model might be different from those in human hypertensive heart disease. Further studies are necessary to clarify complete neural circuits that are involved in

NLRP3 inflammasome activation in hypertensive heart disease. In addition, it has been shown that pathological stress modulates cardiac innervation,[50] although we observed no significant differences in cardiac innervation of catecholaminergic and primary afferent nerve fibers in the adaptive phase of pressure overload. The impact of changes in cardiac innervation patterns on NLRP3 inflammasome activation needs to be elucidated in the future studies.

In conclusion, NLRP3 inflammasome activation through heart-brain interaction initiates cardiac inflammation and hypertrophy during pressure overload. The NLRP3 inflammasome is involved in various diseases including atherosclerosis and metabolic disease.[24] Since the CNS and the SNS control the whole body, our proposed mechanism might also act in NLRP3 inflammasome-related diseases. The nervous system could be a therapeutic target for these diseases, although fine-tuning might be necessary.

SUPPLEMENTAL FIGURES

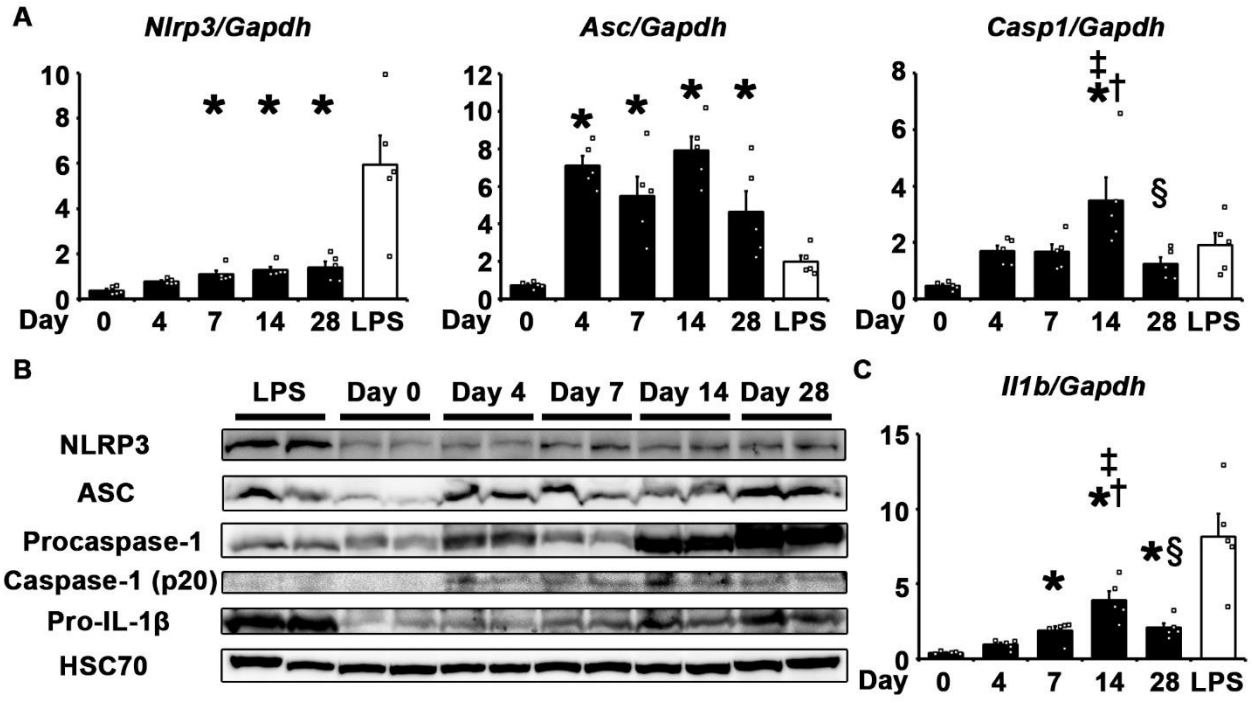

Supplemental Figure 1. NLRP3 Inflammasome Priming and Activation in the Pressure-Overloaded Heart.

A, Time-course gene expression of inflammasome components, such as NLRP3 (*Nlrp3*), the apoptosis-associated speck-like protein containing a C-terminal caspase recruitment domain (*Asc*), and procaspase-1 (*Casp1*) during pressure overload in wild-type (WT) mice (n=5 per group). Quantitative RT-PCR was performed. Expression level of each gene was normalized to that of *Gapdh*. **B,** Western blot for NLRP3, ASC, procapase-1, cleaved caspase-1 (p20), pro-interleukin-1β (pro-IL-1β), and heat shock cognate protein 70 (HSC70) in pressure-overloaded WT hearts. HSC70 served as a loading control. **C,** Time course of *Il1β* gene expression during pressure overload in WT mice (n=5 per group). Quantitative RT-PCR was performed. Expression level of each gene was normalized to that of *Gapdh*. Myocardial samples harvested six hours after intraperitoneal injection of lipopolysaccharide (LPS) were used as positive controls for NLRP3,

ASC, procaspase-1, and pro-IL-1β. *P* values were calculated by one-way ANOVA with Holm test. *$P<0.05$ versus day 0; †$P<0.05$ versus day 4; ‡$P<0.05$ versus day 7; §$P<0.05$ versus day 14. All error bars represent S.E.M.

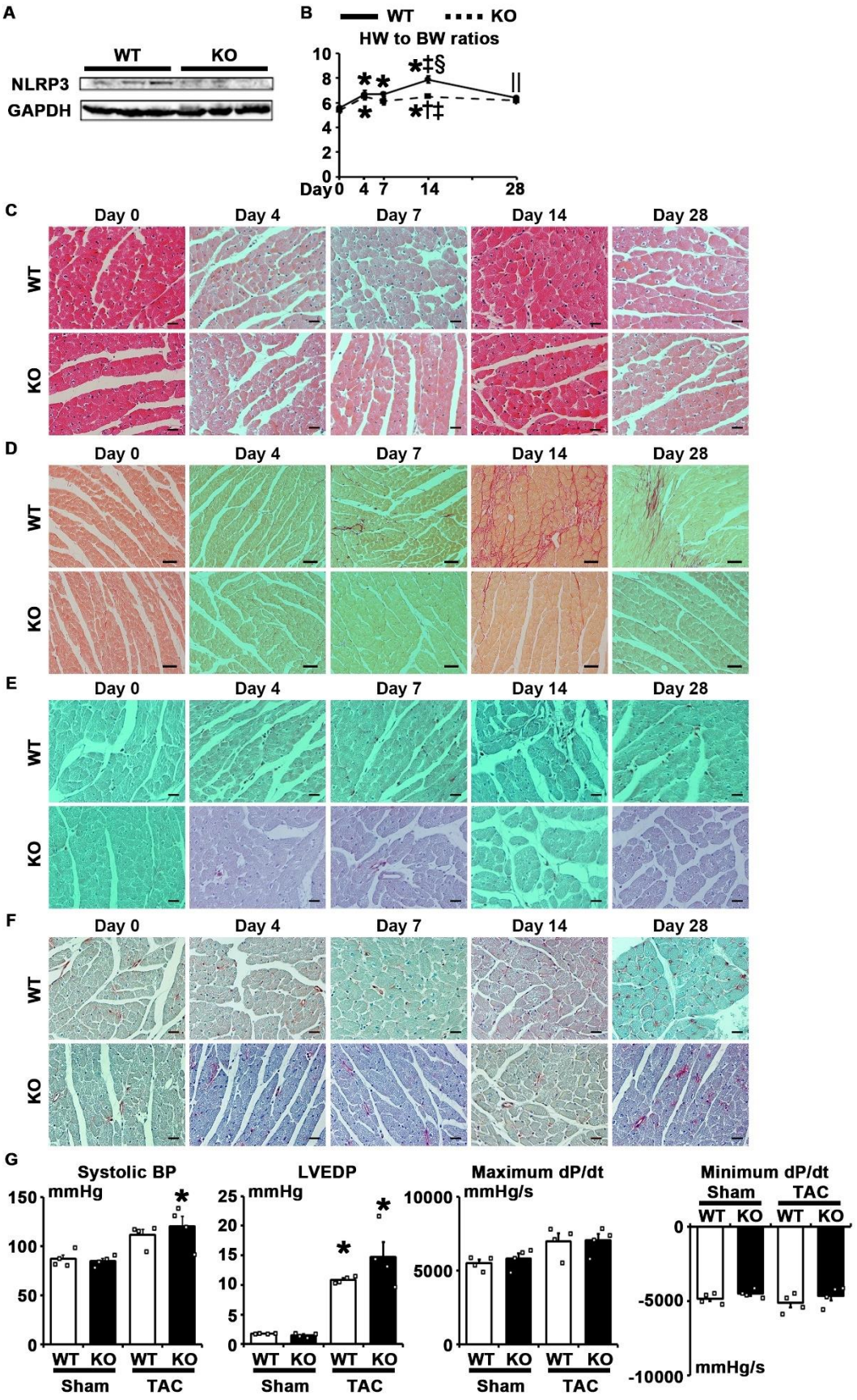
A
WT
KO
NLRP3
GAPDH
B
WT
KO
HW to BW ratios
Day 0 4 7 14 28
C
D
E
F
Day 0
Day 4
Day 7
Day 14
Day 28
WT
KO
G
Systolic BP
mmHg
LVEDP
mmHg
Maximum dP/dt
mmHg/s
Minimum dP/dt
Sham
TAC
WT KO WT KO
Sham TAC

Supplemental Figure 2. NLRP3 Inflammasome Is Involved in Cardiac Adaptive Response During Pressure Overload.

A, Western blot for NLRP3 and glyceradldehyde-3-phosphate dehydrogenase (GAPDH) in WT and *Nlrp3* knockout (KO) hearts. **B,** Time course of heart weight (HW) to body weight (BW) ratio in WT and KO mice during pressure overload (n=5 per group). **C** through **F,** Representative images of hematoxylin and eosin staining (**C**), sirius red staining (**D**), and immunohistochemical staining for Mac3 (**E**) and CD31 (**F**) in WT and KO mice subjected to TAC. These images were used for assessment of cardiomyocyte cross-sectional area (**C**), collagen volume fraction (**D**), macrophage density (**E**), and capillary density (**F**), respectively. Scale bars=20μm for (**C**, **E**, and **F**). Scale bars=50μm for (**D**). **G,** Hemodynamic parameters in WT and KO hearts subjected to sham or 28 days of TAC (n=4 per group). BP, blood pressure; LVEDP, left ventricle end-diastolic pressure. *P* values were calculated by one-way ANOVA with Holm test. For **B**, **P*<0.05 versus day 0; †*P*<0.05 versus WT mice at same time point; ‡*P*<0.05 versus day 4; §*P*<0.05 versus day 7; ‖*P*<0.05 versus day 14. For **G**, **P*<0.05 versus sham. All error bars represent S.E.M.

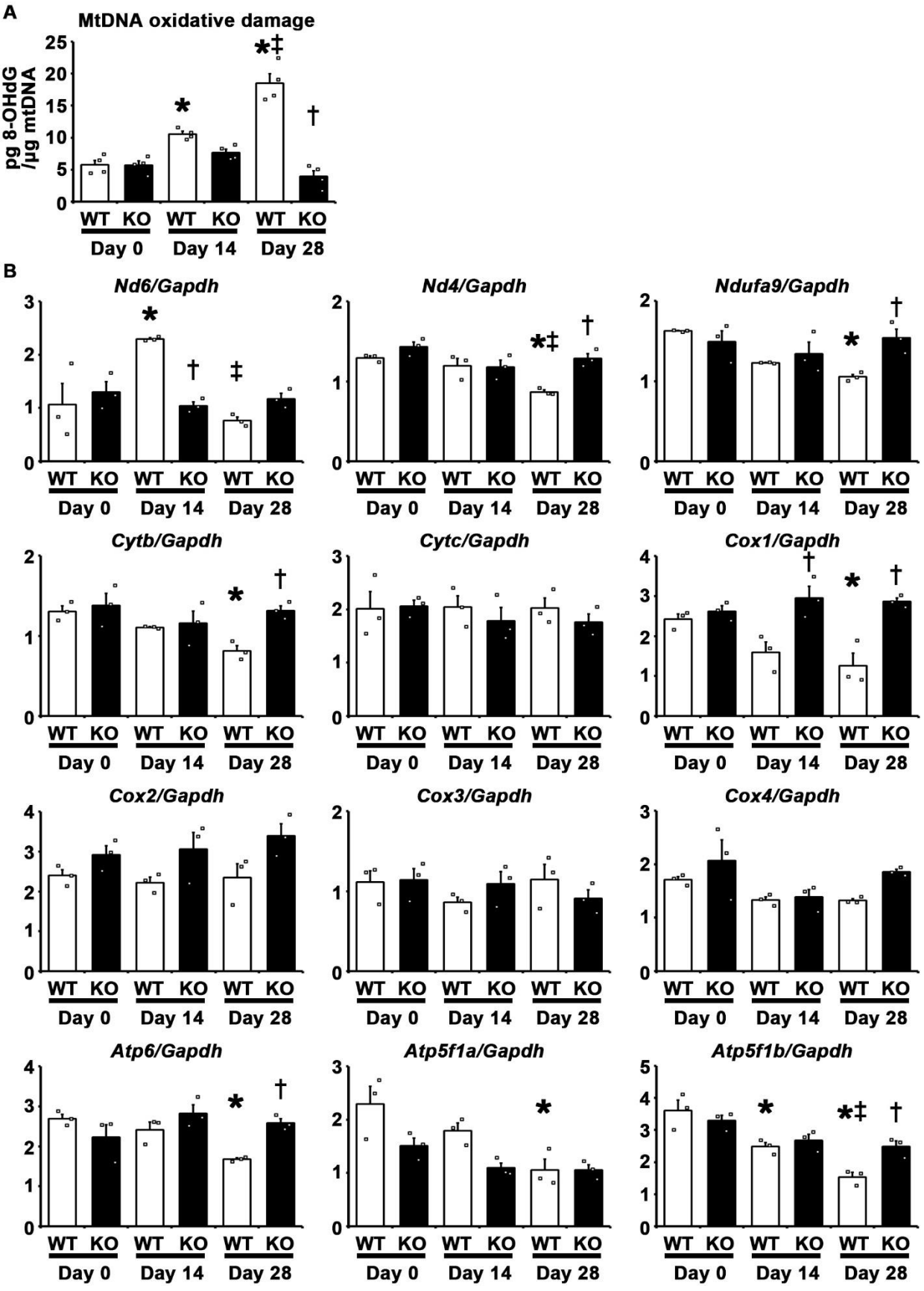
A
MtDNA oxidative damage
pg 8-OHdG /µg mtDNA
WT KO WT KO WT KO
Day 0 Day 14 Day 28
B
Nd6/Gapdh
Nd4/Gapdh
Ndufa9/Gapdh
Cytb/Gapdh
Cytc/Gapdh
Cox1/Gapdh
Cox2/Gapdh
Cox3/Gapdh
Cox4/Gapdh
Atp6/Gapdh
Atp5f1a/Gapdh
Atp5f1b/Gapdh

Supplemental Figure 3. Oxidative Damage of Mitochondrial DNA (mtDNA) and Expression of Genes Associated with Mitochondrial Oxidative Phosphorylation in Pressure-Overloaded Wild-type (WT) and *Nlrp3* Knockout (KO) Hearts.

A, Oxidative damage of mtDNA in the heart (n=4 per group). Measurement of 8-hydroxy-2'-deoxyguanine (8-OHdG) level in mtDNA isolated from WT and KO hearts was performed. Values were normalized to mtDNA level. **B,** Expression levels of genes associated with mitochondrial oxidative phosphorylation, such as NADH-ubiquinone oxidoreductase chain 6 (*Nd6*), *Nd4*, NADH:ubiquinone oxidoreductase subunit A9 (*Ndufa9*), cytochrome b (*Cytb*), cytochrome c (*Cytc*), cytochrome c oxidase subunit I (Cox1), *Cox2*, *Cox3*, *Cox4*, ATPase-6 (*Atp6*), ATP synthase F1 subunit alpha (*Atp5f1a*), and *Atp5f1b*, in WT and KO hearts (n=3 per group). Quantitative RT-PCR was performed. Expression level of each gene was normalized to that of *Gapdh*. *P* values were calculated by one-way ANOVA with Holm test. **P*<0.05 versus day 0; †*P*<0.05 versus WT mice; ‡*P*<0.05 versus day 14. All error bars represent S.E.M.

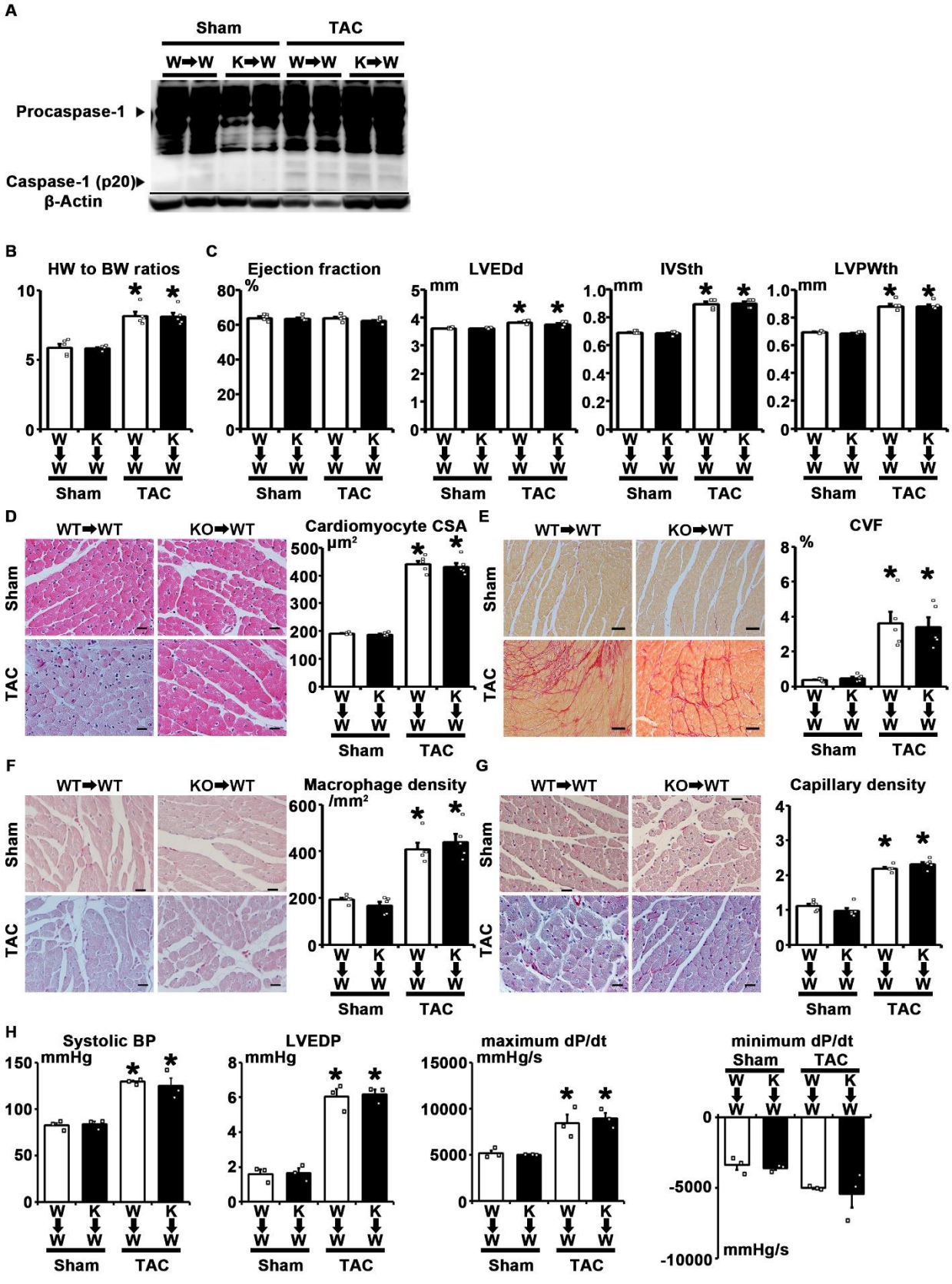
A
Sham
TAC
W➡W
K➡W
W➡W
K➡W
Procaspase-1
Caspase-1 (p20)
β-Actin
B
HW to BW ratios
C
Ejection fraction
LVEDd
IVSth
LVPWth
Sham
TAC
D
WT➡WT
KO➡WT
Cardiomyocyte CSA
E
CVF
F
Macrophage density
G
Capillary density
H
Systolic BP
LVEDP
maximum dP/dt
minimum dP/dt
mmHg
mmHg/s

1

Supplemental Figure 4. NLRP3 Expressed in Bone Marrow-Derived Cells Has Little Impact on Initiation of Cardiac Inflammation and Cardiac Hypertrophy.

A through **H,** Wild-type mice with wild-type bone marrow (W→W) or *Nlrp3* knockout bone marrow (K→W) were subjected to sham or 14 days of TAC. **A,** Western blot for procapase-1, cleaved caspase-1 (p20), and β-actin in the heart. **B,** Heart weight (HW) to body weight (BW) ratio (n=5 per group). **C,** Echocardiographic analysis of ejection fraction, left ventricle end-diastolic diameter (LVEDd), interventricular septum thickness (IVSth), and left ventricular posterior wall thickness (LVPWth) (n=5 per group). **D** through **G,** Histological analysis of cardiomyocyte cross-sectional area (CSA) (**D**), collagen volume fraction (CVF) (**E**), macrophage density (**F**) and capillary density (**G**) (n=5 per group). Quantification of cardiomyocyte CSA and CVF was performed in specimens stained with hematoxylin and eosin or sirius red dye, respectively. Quantification of macrophage and capillary density was performed by immunohistochemical staining for Mac3 and CD31, respectively. Representative images are shown for each analysis. Scale bars=20μm for (**D**, **F**, and **G**). Scale bars=50μm for (**E**). **H,** Hemodynamic parameters (n=3 per group). BP, blood pressure; LVEDP, left ventricle end-diastolic pressure. *P* values were calculated by one-way ANOVA with Holm test. **P*<0.05 versus sham. All error bars represent S.E.M.

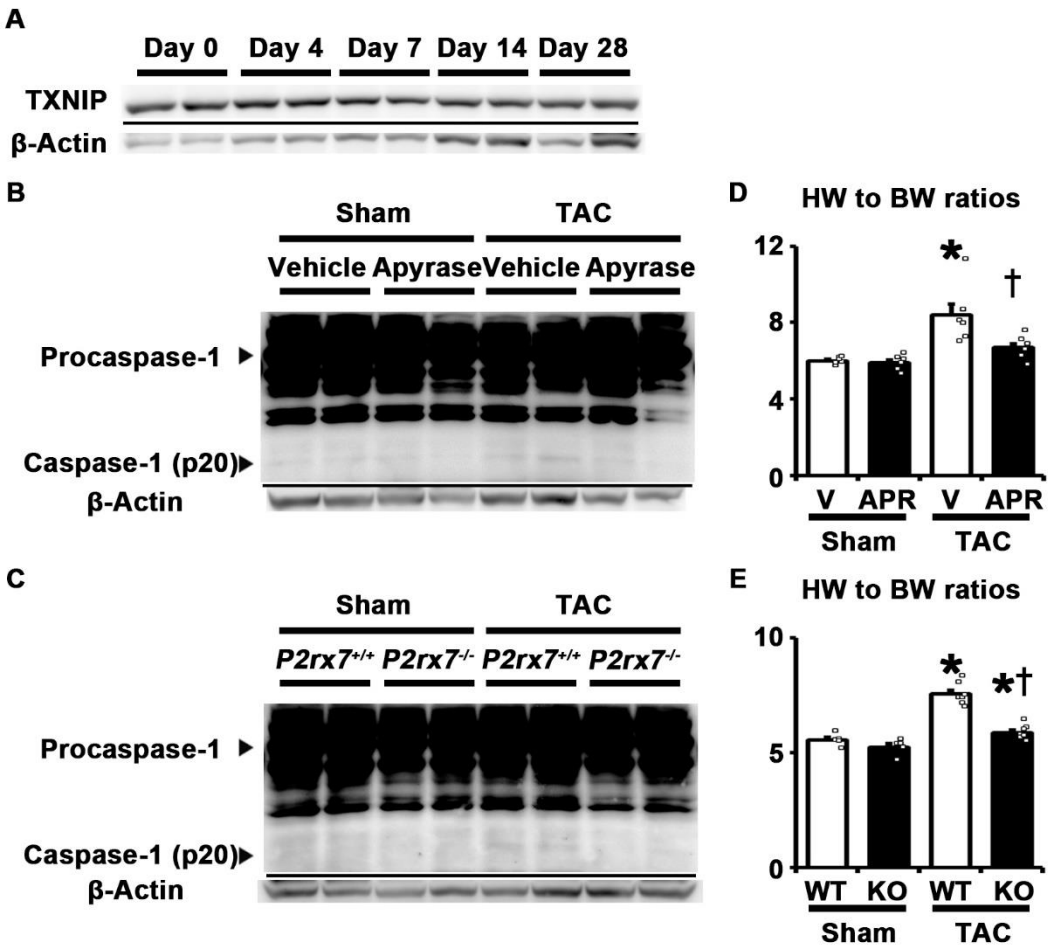

Supplemental Figure 5. Extracellular ATP and P2X7 Purinergic Receptor Are Involved in NLRP3 Inflammasome Activation in the Pressure-Overloaded Heart.

A, Western blot for thioredoxin-interacting protein (TXNIP) and β-actin in wild-type (WT) hearts during pressure overload. **B,** Western blot for procapase-1, cleaved caspase-1 (p20), and β-actin in vehicle-treated (V) or apyrase-treated (APR) WT hearts subjected to sham or 14 days of TAC. **C,** Western blot for procapase-1, cleaved caspase-1 (p20), and β-actin in WT and *P2rx7* knockout (KO) hearts subjected to sham or 14 days of TAC. **D,** Heart weight (HW) to body weight (BW) ratio in V or APR hearts subjected to sham or 14 days of TAC (n=6 for sham; n=7 for TAC). **E,** HW to BW ratio in WT and KO hearts subjected to sham or 14 days of TAC (n=5 for sham; n=7

for TAC). *P* values were calculated by one-way ANOVA with Holm test. *$P<0.05$ versus sham. †$P<0.05$ versus V or WT mice. All error bars represent S.E.M.

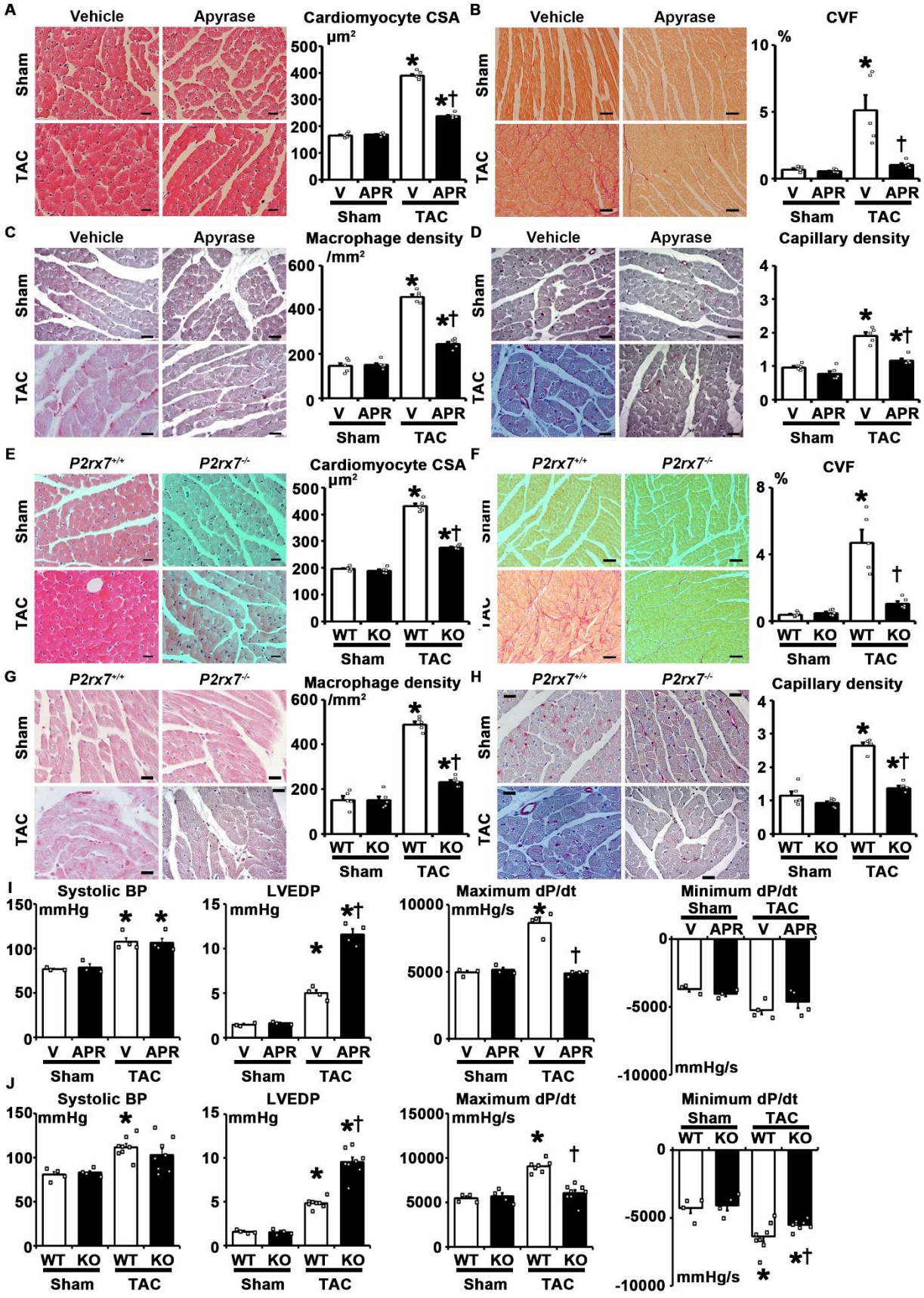
A
Vehicle
Apyrase
Sham
TAC
Cardiomyocyte CSA
µm²
V APR V APR
Sham TAC
B
CVF
%
C
Macrophage density
/mm²
D
Capillary density
E
P2rx7+/+
P2rx7-/-
WT KO WT KO
F
G
H
I
Systolic BP
mmHg
LVEDP
Maximum dP/dt
mmHg/s
Minimum dP/dt
J

Supplemental Figure 6. Extracellular ATP Depletion by ATP Diphosphohydrolase, Apyrase, or Genetic Disruption of P2X7 Purinergic Receptor Leads to Impairment of Adaptive Cardiac Hypertrophy During Pressure Overload.

A through **D,** Histological analysis of cardiomyocyte cross-sectional area (CSA) (**A**), collagen volume fraction (CVF) (**B**), macrophage density (**C**) and capillary density (**D**) in vehicle-treated (V) or apyrase-treated (APR) wild-type (WT) mice subjected to sham or 14 days of TAC (n=5 per group). **E** through **H,** Histological analysis of cardiomyocyte CSA (**E**), CVF (**F**), macrophage density (**G**) and capillary density (**H**) in WT and *P2rx7* knockout (KO) mice subjected to sham or 14 days of TAC (n=5 per group). Quantification of cardiomyocyte CSA and CVF was performed in specimens stained with hematoxylin and eosin or sirius red dye, respectively. Quantification of macrophage and capillary density was performed by immunohistochemical staining for Mac3 and CD31, respectively. Representative images are shown for each analysis. Scale bars=20μm for (**A**, **C**, **D**, **E**, **G**, and **H**). Scale bars=50μm for (**B** and **F**). **I,** Hemodynamic parameters in V or APR mice subjected to sham or 14 days of TAC (n=3 for sham; n=4 for TAC). **J,** Hemodynamic parameters in WT and KO mice subjected to sham or 14 days of TAC (n=4 for sham; n=8 for TAC). BP, blood pressure; LVEDP, left ventricle end-diastolic pressure. *P* values were calculated by one-way ANOVA with Holm test. **P*<0.05 versus sham. †*P*<0.05 versus V or WT mice. All error bars represent S.E.M.

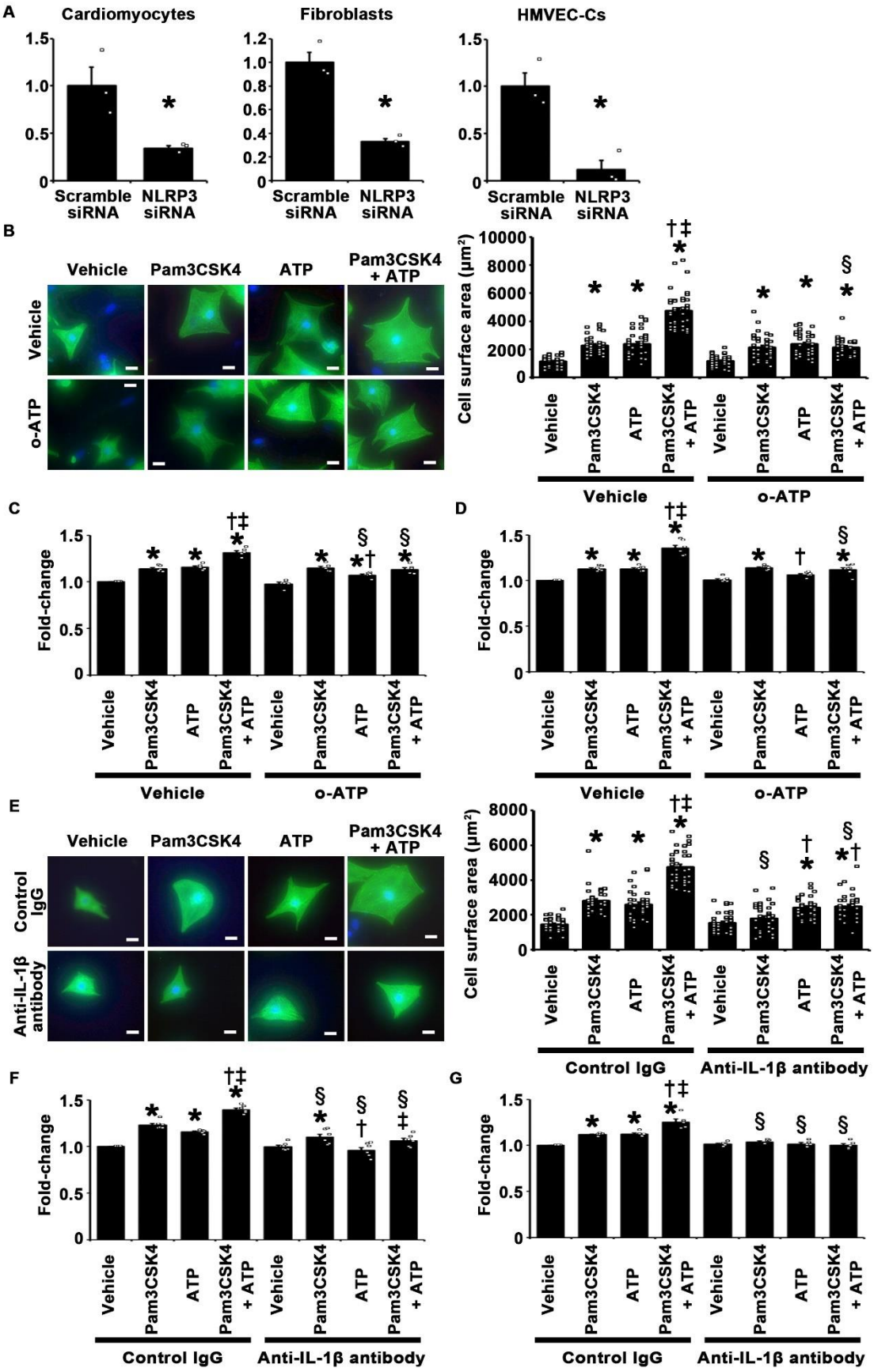
A
Cardiomyocytes
Fibroblasts
HMVEC-Cs
Scramble siRNA
NLRP3 siRNA
B
Vehicle
Pam3CSK4
ATP
Pam3CSK4 + ATP
o-ATP
Cell surface area (μm²)
C
D
Fold-change
E
Control IgG
Anti-IL-1β antibody
F
G

Supplemental Figure 7. Pharmacological Inhibition of P2X7 Purinergic Receptor or Anti-IL-1β Neutralization Antibody Treatment Suppresses Synergistic Effects of ATP and Pam3CSK4 on Cardiomyocyte Hypertrophy and Proliferation of Fibroblasts and Vascular Endothelial Cells.

A, Knockdown efficiency of NLRP3 siRNA in cardiomyocytes, fibroblasts, and human microvascular endothelial cells from the heart (HMVEC-C) (n=3 per group). Gene expression level of *Nlrp3* was assessed by quantitative RT-PCR, and normalized to that of *Gapdh*. **B** through **D,** Cell surface area of cardiomyocytes after 48-hour stimulation (n=40 per group) (**B**) and proliferation of cardiac fibroblasts (n=5 per group) (**C**) and HMVEC-C (n=6 per group) (**D**) after 24-hour stimulation with Pam3CSK4, ATP, or both under treatment with vehicle or oxidized ATP (o-ATP), a P2X7 receptor antagonist. Scale bars=20μm. **E** through **G**, Cell surface area of cardiomyocytes after 48-hour stimulation (n=40 per group) (**E**) and proliferation of cardiac fibroblasts (n=6 per group) (**F**) and HMVEC-C (n=5 per group) (**G**) after 24-hour stimulation with Pam3CSK4, ATP, or both under treatment with control IgG or anti-IL-1β antibody. Scale bars=20μm. Cell surface area of cardiomyocytes was measured in specimens by anti-sarcomeric α-actinin staining. Cell proliferation was assessed by MTS (dimethylthiazol-carboxymethoxyphenyl-sulfophenyl-tetrazolium) assay. The percentage of the absorbance of wells with cells treated with vehicle for o-ATP and vehicle for stimulants (**C** and **D**) or wells with cells treated with control IgG or vehicle (**F** and **G**) was calculated. Data are expressed as a fold-change relative to the control group. *P* values were calculated by unpaired two-tailed t-test (**A**) or one-way ANOVA with Holm test (**B** through **G**). For **A**, **P*<0.05 versus scrambled siRNA. For **B** through **D**, **P*<0.05 versus vehicle for stimulants; †*P*<0.05 versus Pam3CSK4; ‡*P*<0.05 versus ATP; §*P*<0.05 versus vehicle for o-ATP. For **E** through **G**, **P*<0.05 versus vehicle; †*P*<0.05

versus Pam3CSK4; ‡P<0.05 versus ATP; §P<0.05 versus control IgG. All error bars represent S.E.M.

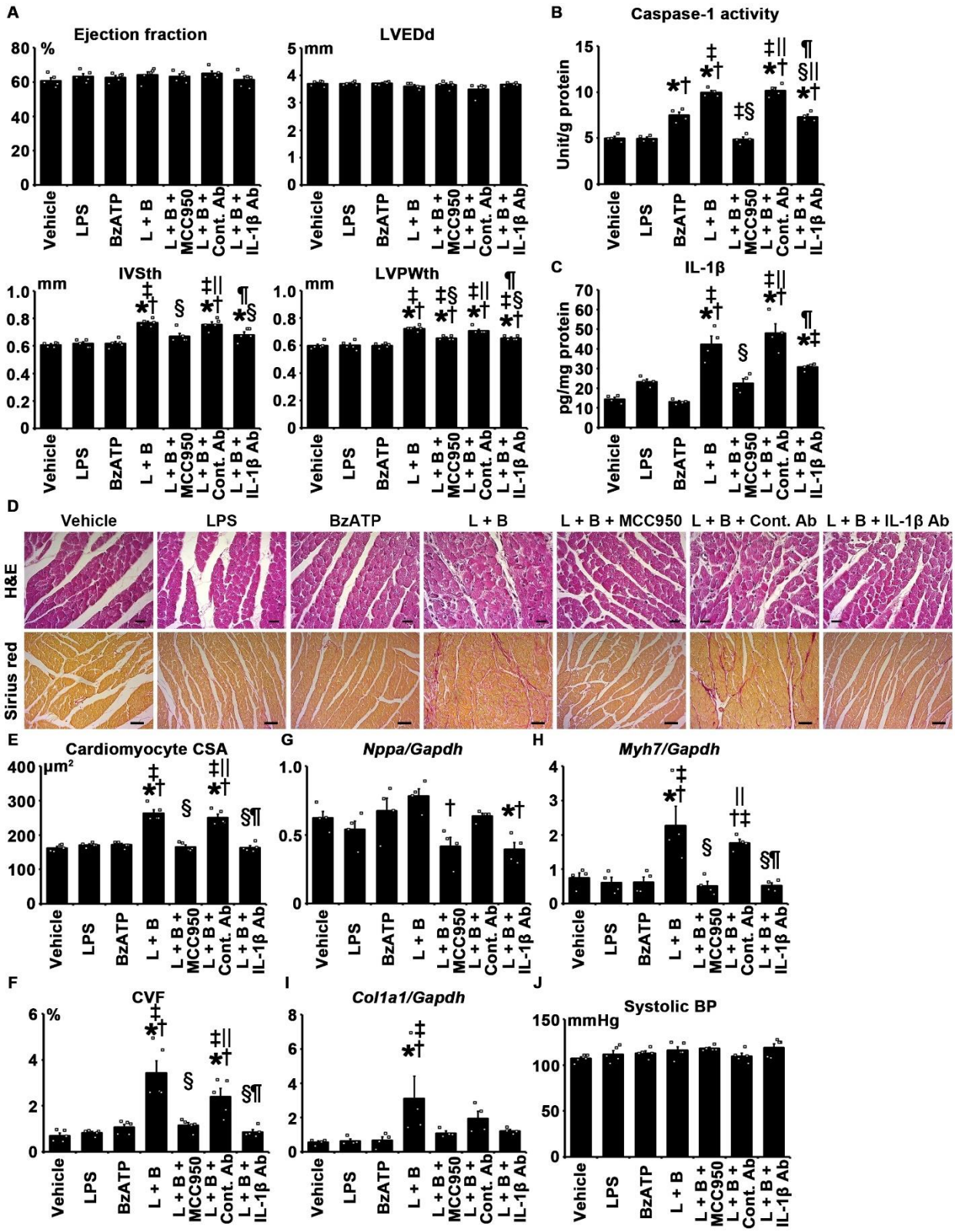
A
Ejection fraction
%
LVEDd
mm
IVSth
mm
LVPWth
mm
B
Caspase-1 activity
Unit/g protein
C
IL-1β
pg/mg protein
D
Vehicle
LPS
BzATP
L + B
L + B + MCC950
L + B + Cont. Ab
L + B + IL-1β Ab
H&E
Sirius red
E
Cardiomyocyte CSA
μm²
G
Nppa/Gapdh
H
Myh7/Gapdh
F
CVF
%
I
Col1a1/Gapdh
J
Systolic BP
mmHg

Supplemental Figure 8. Pharmacological Stimulation of P2X7 Purinergic Receptor, in Combination with Inflammasome Priming Signal by Lipopolysaccharide, Induces Cardiac Hypertrophy Through NLRP3 Inflammasome Activation and IL-1β Production *in Vivo*.

A through **J,** Wild-type mice were treated with lipopolysaccharide (LPS), 2'(3')-O-(4-benzoylbenzoyl)-ATP (BzATP), a combination of LPS and BzATP (LPS+BzATP), or vehicle for 14 days. Wild-type mice treated with the combination were additionally treated with a potent and specific NLRP3 inhibitor (MCC950) (LPS+BzATP+MCC950), anti-IL-1β antibodies (LPS+BzATP+IL-1β Ab), or control antibodies (LPS+BzATP+Cont. Ab). **A,** Echocardiographic analysis of left ventricle end-diastolic diameter (LVEDd), interventricular septum thickness (IVSth), and left ventricular posterior wall thickness (LVPWth) (n=5 per group). **B** and **C,** Myocardial caspase-1 activity (**B**) and IL-1β protein level (**C**) (n=4 per group). IL-1β protein was detected by ELISA. Values were normalized to total protein level. **D,** Representative images of hematoxylin and eosin (H&E) and sirius red staining. Scale bars=20μm for H&E. Scale bars=50μm for sirius red. **E** and **F,** Histological analysis of cardiomyocyte cross-sectional area (CSA) (**E**) and collagen volume fraction (**F**) (n=5 per group). Quantification of cardiomyocyte CSA and CVF was performed in specimens stained with H&E or sirius red dye, respectively. **G** and **H,** Expression levels of hypertrophic marker genes, such as *Nppa* (**G**) and *Myh7* (**H**), and a fibrosis-related gene, such as *Col1a1* (**I**), in the heart (n=4 per group). **J,** Systolic blood pressure (n=5 per group). *P* values were calculated by one-way ANOVA with Holm test. For **A** through **C**, **E**, **F**, **H**, and **I,** **P*<0.05 versus vehicle; †*P*<0.05 versus LPS; ‡*P*<0.05 versus BzATP; §*P*<0.05 versus LPS+BzATP; ‖*P*<0.05 versus LPS+BzATP+MCC950; ¶*P*<0.05 versus LPS+BzATP+Cont. Ab. For **G**, **P*<0.05 versus BzATP; †*P*<0.05 versus L+B. All error bars represent S.E.M.

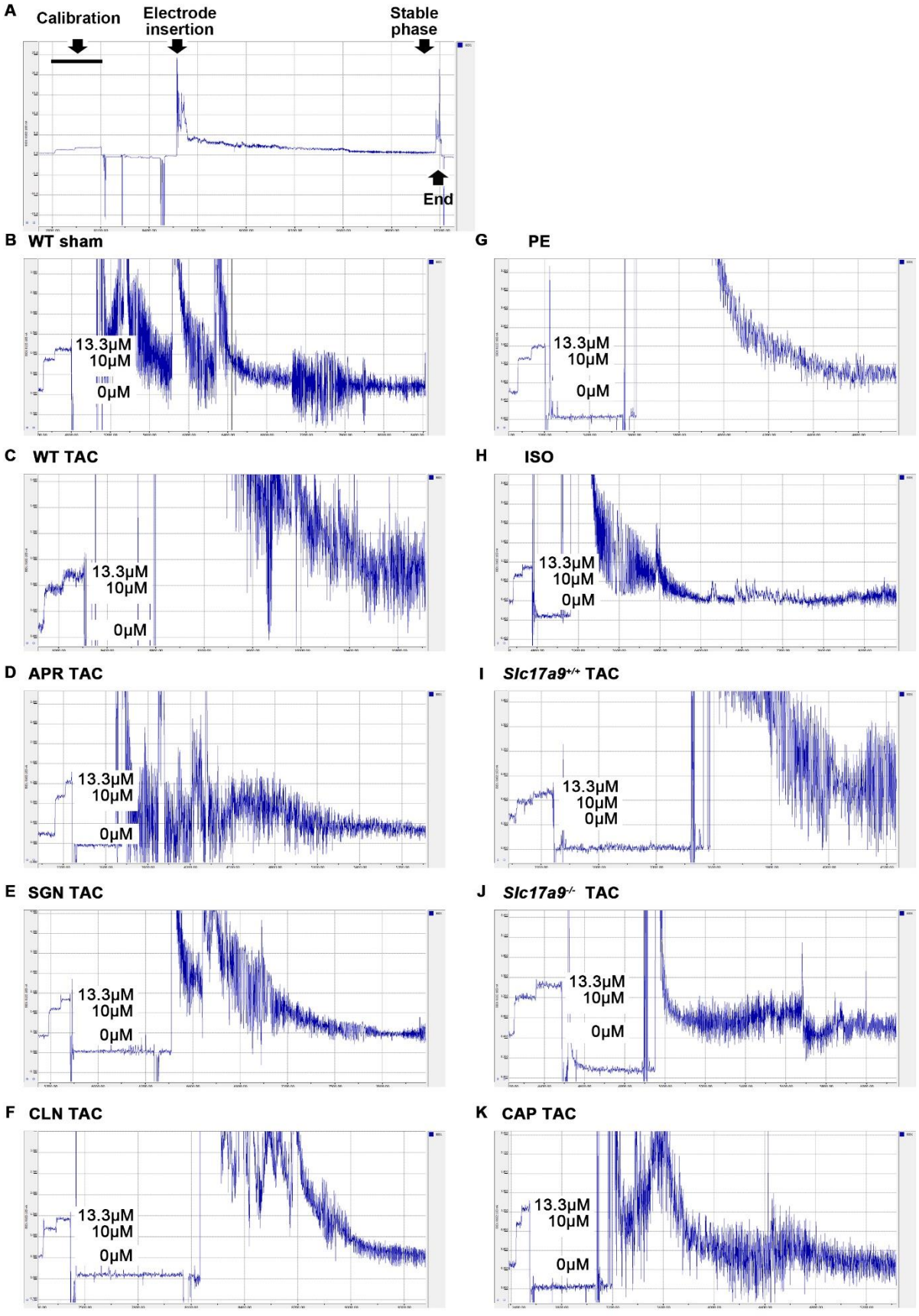
A
Calibration
Electrode insertion
Stable phase
End
B WT sham
13.3μM
10μM
0μM
C WT TAC
13.3μM
10μM
0μM
D APR TAC
13.3μM
10μM
0μM
E SGN TAC
13.3μM
10μM
0μM
F CLN TAC
13.3μM
10μM
0μM
G PE
13.3μM
10μM
0μM
H ISO
13.3μM
10μM
0μM
I Slc17a9+/+ TAC
13.3μM
10μM
0μM
J Slc17a9-/- TAC
13.3μM
10μM
0μM
K CAP TAC
13.3μM
10μM
0μM

1

Supplemental Figure 9. Extracellular ATP Measurement in Heart *in Vivo*.

A, Representative image of ATP measurement with the ATP biosensor system. Electric current between the reference electrode and the ATP biosensor was measured through a potentiostat and transformed into ATP level based on the calibration curve. Calibration was performed using ATP solution just before the insertion of the reference electrode and the ATP biosensor. Insertion of the reference electrode and the ATP biosensor causes tissue injury, which leads to massive release of intracellular ATP from damaged cells into the extracellular space. To eliminate the influence of tissue injury, ATP level in the stable phase, in which the tendency of detected electric currents does not change, was measured as extracellular ATP concentration. Extracellular ATP level was calculated by averaging ATP levels at 60 time points (i.e. 60 seconds) in the stable phase. Three mice were analyzed for each group. **B** through **K,** Representative images of data of ATP measurement in the heart in sham-operated mice (WT sham) (**B**), TAC-operated mice (WT TAC) (**C**), TAC-operated mice with left stellate ganglionectomy (SGN TAC) (**D**), pseudoephedrine-treated mice (PE) (**E**), isoproterenol-treated mice (ISO) (**F**), and TAC-operated mice treated with apyrase (APR TAC) (**G**), clonidine (CLN TAC) (**H**), or capsaicin (CAP TAC) (**I**), *Slc17a9*$^{flox/flox}$;DBH-*Cre*$^{-}$ mice (CWT TAC) (**J**), and *Slc17a9*$^{flox/flox}$;DBH-*Cre*$^{+}$ mice (CKO TAC) (**K**). Mice were subjected to sham or 14 days of TAC.

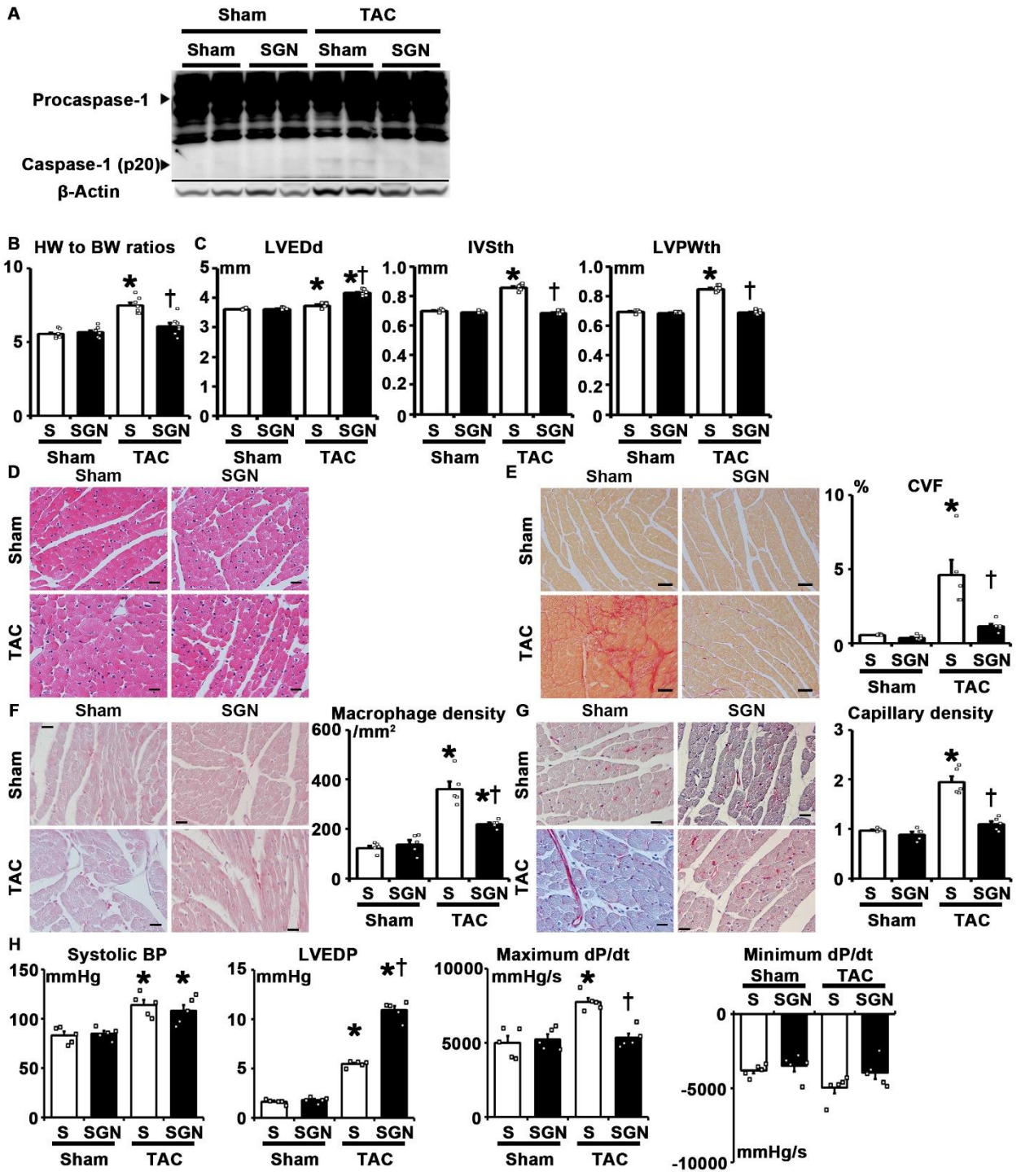

Supplemental Figure 10. Left Stellate Ganglionectomy (SGN) Inhibits Adaptive Cardiac Hypertrophy During Pressure Overload.

A through **H,** Wild-type mice with sham (S) or SGN were subjected to sham or 14 days of TAC. **A,** Western blot for procapase-1, cleaved caspase-1 (p20), and β-actin in the heart. **B,** Heart weight (HW) to body weight (BW) ratio (n=7 per group). **C,** Echocardiographic analysis of left ventricle end-diastolic diameter (LVEDd), interventricular septum thickness (IVSth), and left ventricular posterior wall thickness (LVPWth) (n=7 per group). **D,** Representative images of hematoxylin and eosin staining. Scale bars=20μm. **E** through **G,** Histological analysis of collagen volume fraction (CVF) (**E**), macrophage density (**F**) and capillary density (**G**) (n=5 per group). Quantification of CVF was performed in specimens stained with sirius red dye. Quantification of macrophage and capillary density was performed by immunohistochemical staining for Mac3 or CD31, respectively. Representative images are shown for each analysis. Scale bars=50μm for (**E**). Scale bars=20μm for (**F** and **G**). **H,** Hemodynamic parameters (n=5 per group). BP, blood pressure; LVEDP, left ventricle end-diastolic pressure. *P* values were calculated by one-way ANOVA with Holm test. **P*<0.05 versus sham for TAC. †*P*<0.05 versus sham for SGN. All error bars represent S.E.M.

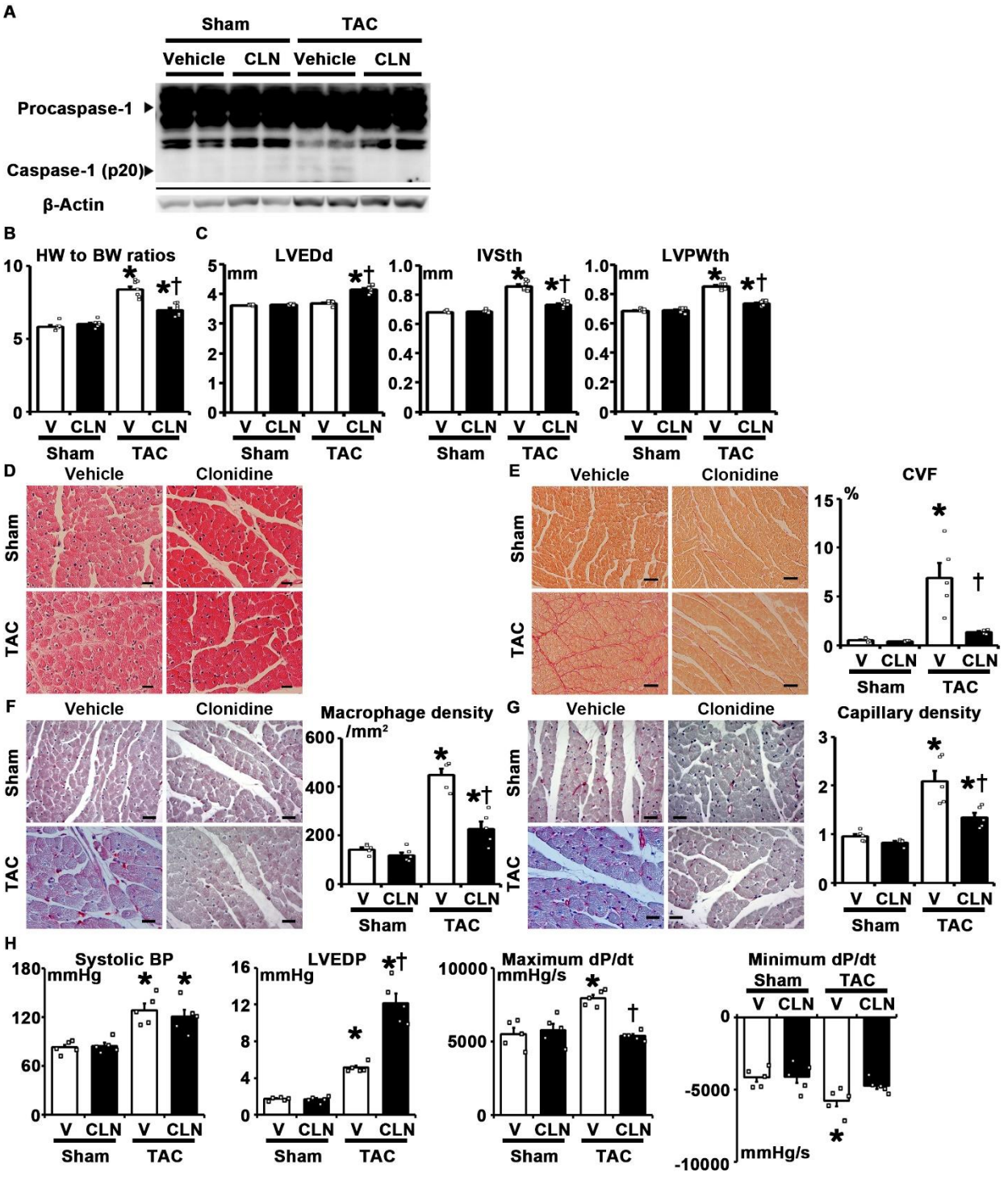

Supplemental Figure 11. Clonidine (CLN) Treatment Inhibits Adaptive Cardiac Hypertrophy During Pressure Overload.

A through **H,** Wild-type mice with vehicle (V) or CLN treatment were subjected to sham or 14 days of TAC. **A,** Western blot for procapase-1, cleaved caspase-1 (p20), and β-actin in the heart. **B,** Heart weight (HW) to body weight (BW) ratio (n=6 for sham; n=7 for TAC). **C,** Echocardiographic analysis of left ventricle end-diastolic diameter (LVEDd), interventricular septum thickness (IVSth), and left ventricular posterior wall thickness (LVPWth) (n=6 for sham; n=7 for TAC). **D,** Representative images of hematoxylin and eosin staining. Scale bars=20μm. **E** through **G**, Histological analysis of collagen volume fraction (CVF) (**E**), macrophage density (**F**) and capillary density (**G**) (n=5 per group). Quantification of CVF was performed in specimens stained with sirius red dye. Quantification of macrophage and capillary density was performed by immunohistochemical staining for Mac3 or CD31, respectively. Representative images are shown for each analysis. Scale bars=50μm for (**E**). Scale bars=20μm for (**F** and **G**). **H,** Hemodynamic parameters (n=5 per group). BP, blood pressure; LVEDP, left ventricle end-diastolic pressure. *P* values were calculated by one-way ANOVA with Holm test. **P*<0.05 versus sham. †*P*<0.05 versus vehicle. All error bars represent S.E.M.

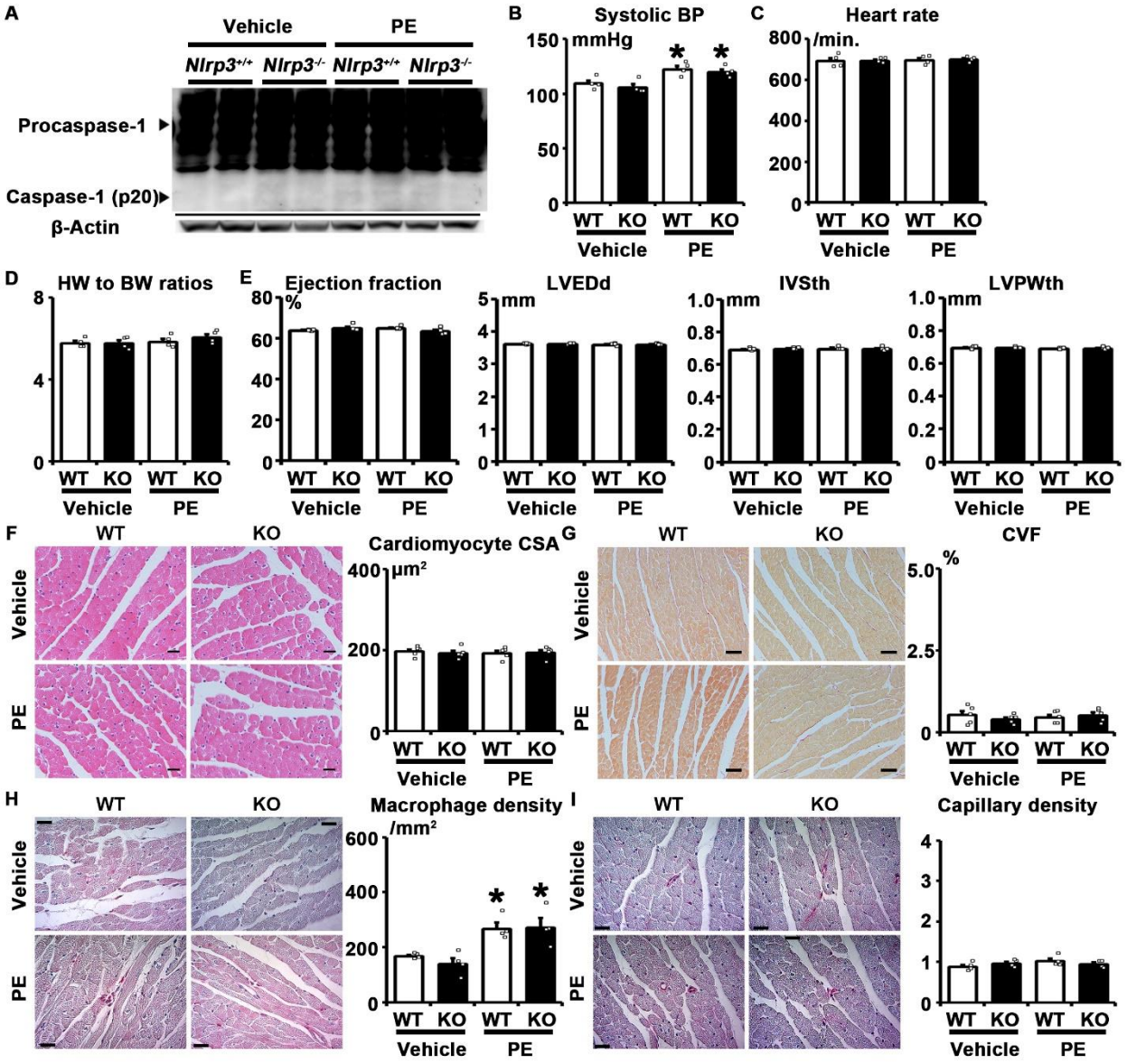

Supplemental Figure 12. Impact of Pseudoephedrine (PE) on Wild-type (WT) and *Nlrp3* Knockout (KO) Hearts.

A through **I,** WT and KO mice were subjected to 14 days of vehicle or PE treatment. **A,** Western blot for procapase-1, cleaved caspase-1 (p20), and β-actin in the heart. **B** and **C,** Systolic blood pressure (BP) (**B**) and heart rate (**C**) (n=4 per group). **D,** Heart weight (HW) to body weight (BW) ratio (n=4 per group). **E,** Echocardiographic analysis of ejection fraction, left ventricle end-diastolic diameter (LVEDd), interventricular septum thickness (IVSth), and left ventricular

posterior wall thickness (LVPWth) (n=4 per group). **F** through **I,** Histological analysis of cardiomyocyte cross-sectional area (CSA) (**F**), collagen volume fraction (CVF) (**G**), macrophage density (**H**) and capillary density (**I**) (n=5 per group for **F** and **G**; n=4 per group for **H** and **I**). Quantification of cardiomyocyte CSA and CVF was performed in specimens stained with hematoxylin and eosin or sirius red dye, respectively. Quantification of macrophage and capillary density was performed by immunohistochemical staining for Mac3 and CD31, respectively. Representative images are shown for each analysis. Scale bars=20μm for (**F**, **H** and **I**). Scale bars=50μm for (**G**). *P* values were calculated by one-way ANOVA with Holm test. **P*<0.05 versus vehicle. All error bars represent S.E.M.

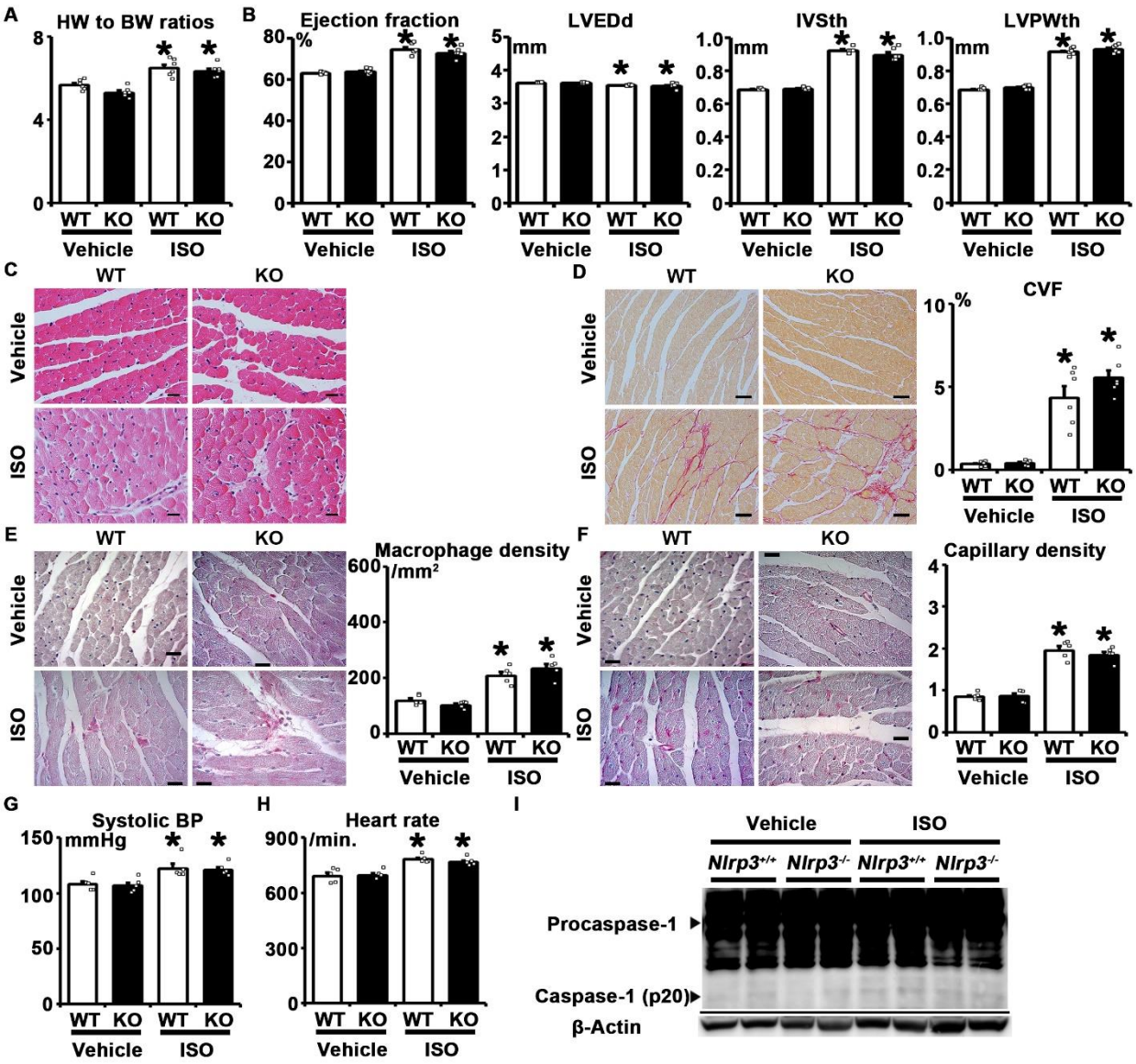

Supplemental Figure 13. Impact of Isoproterenol (ISO) on Wild-type (WT) and *Nlrp3* Knockout (KO) Hearts.

A through **I,** WT and KO mice were subjected to 14 days of vehicle or isoproterenol (ISO) infusion. **A,** Heart weight (HW) to body weight (BW) ratio (n=6 per group). **B,** Echocardiographic analysis of ejection fraction, left ventricle end-diastolic diameter (LVEDd), interventricular septum thickness (IVSth), and left ventricular posterior wall thickness (LVPWth) (n=6 per group). **C,** Representative images of hematoxylin and eosin staining. Scale bars=20μm. **D** through **F,**

Histological analysis of collagen volume fraction (CVF) (**D**), macrophage density (**E**) and capillary density (**F**) (n=6 per group for **D**; n=5 per group for **E** and **F**). Quantification of CVF was performed in specimens stained with sirius red dye. Quantification of macrophage and capillary density was performed by immunohistochemical staining for Mac3 or CD31, respectively. Representative images are shown for each analysis. Scale bars=50μm for (**D**). Scale bars=20μm for (**E** and **F**). **G** and **H,** Systolic blood pressure (BP) (**G**) and heart rate (**H**) (n=5 per group). **I,** Western blot for procapase-1, cleaved caspase-1 (p20), and β-actin in the heart. *P* values were calculated by one-way ANOVA with Holm test. **P*<0.05 versus vehicle. All error bars represent S.E.M.

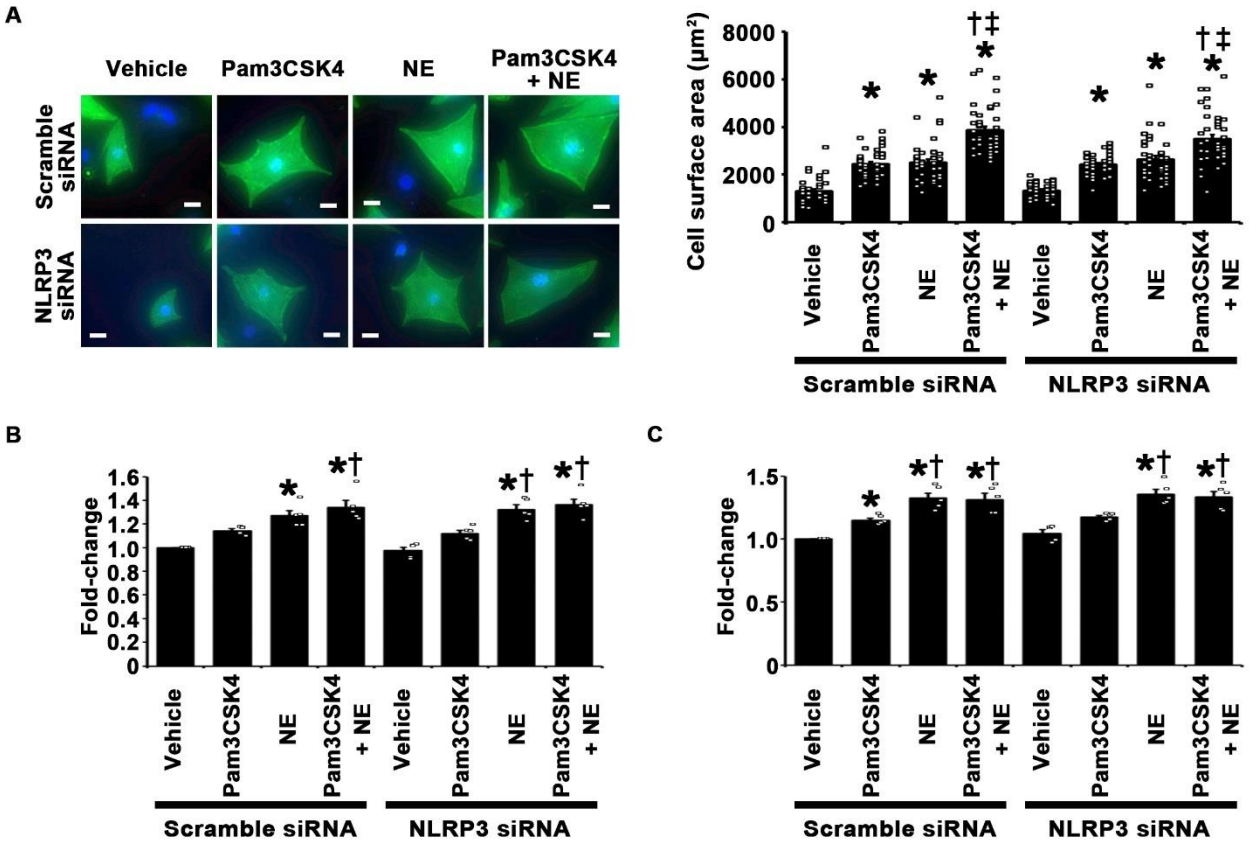

Supplemental Figure 14. Norepinephrine Induces Cardiomyocyte Hypertrophy and Proliferation of Cardiac Fibroblasts and Vascular Endothelial Cells in an NLRP3 Inflammasome-Independent Manner *in Vitro*.

A through **C,** Cell surface area of cardiomyocytes after 48-hour stimulation (n=40 per group) (**A**) and proliferation of cardiac fibroblasts (n=5 per group) (**B**) and human microvascular endothelial cells from the heart (HMVEC-C) (n=5 per group) (**C**) after 24-hour stimulation with Pam3CSK4, norepinephrine (NE), or both under treatment with NLRP3 siRNA or scrambled siRNA. Cell surface area in specimens was measured by anti-sarcomeric α-actinin staining. Scale bars=20μm for (**A**). Cell proliferation was assessed by MTS (dimethylthiazol-carboxymethoxyphenyl-sulfophenyl-tetrazolium) assay, and expressed as the percentage of the absorbance of wells with cells treated with scrambled siRNA or vehicle. *P* values were calculated by one-way ANOVA with

Holm test. *P<0.05 versus vehicle; †P<0.05 versus Pam3CSK4; ‡P<0.05 versus NE. All error bars represent S.E.M.

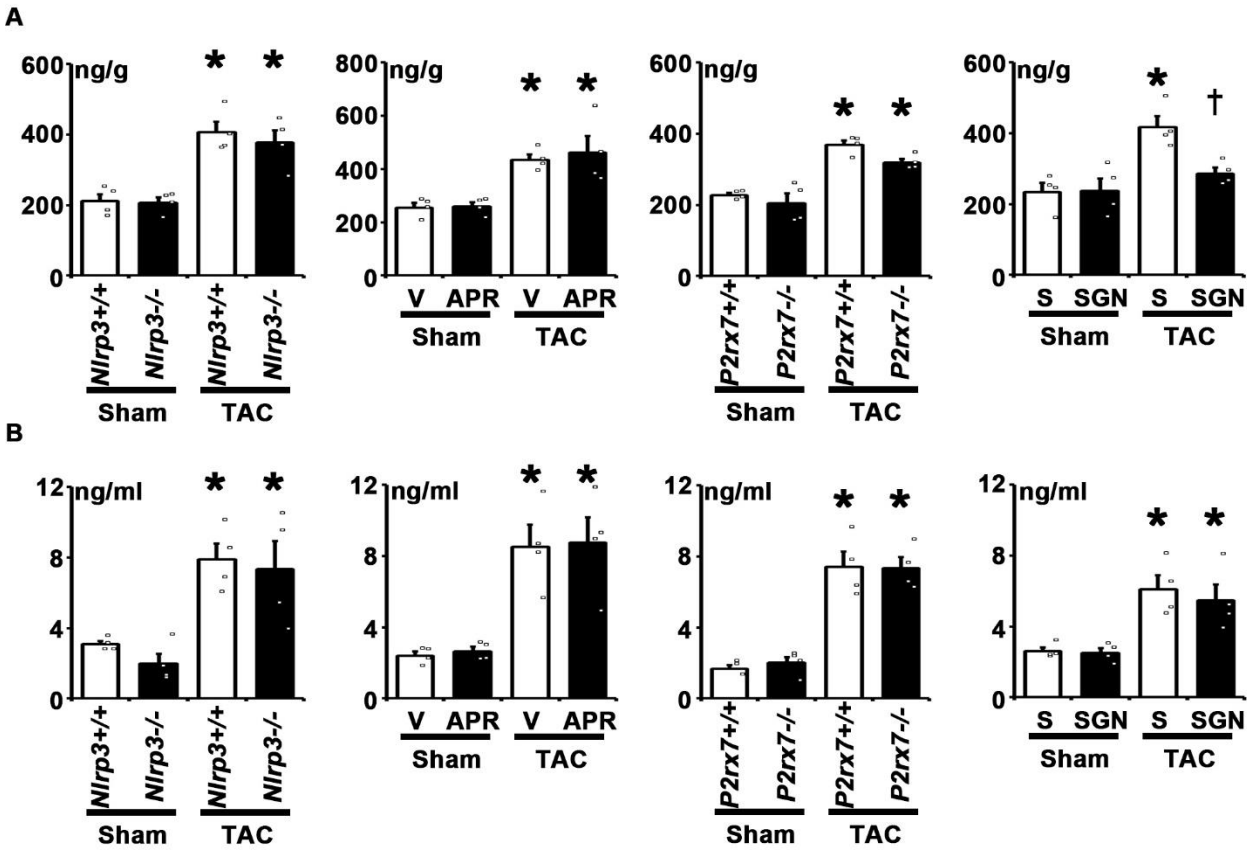

Supplemental Figure 15. Impact of ATP/P2X7 Axis on Myocardial and Plasma Norepinephrine Levels.

A and **B,** Myocardial (**A**) and plasma (**B**) norepinephrine levels in *Nlrp3*$^{-/-}$ mice, *P2rx7*$^{-/-}$ mice, and wild-type mice treated with apyrase (APR) or the left stellate ganglionectomy (SGN) (n=4 per group). Norepinephrine was detected by ELISA. Myocardial norepinephrine levels were normalized to tissue weight. V, vehicle; S, sham for SGN. *P* values were calculated by one-way ANOVA with Holm test. **P*<0.05 versus sham. †*P*<0.05 versus S. All error bars represent S.E.M.

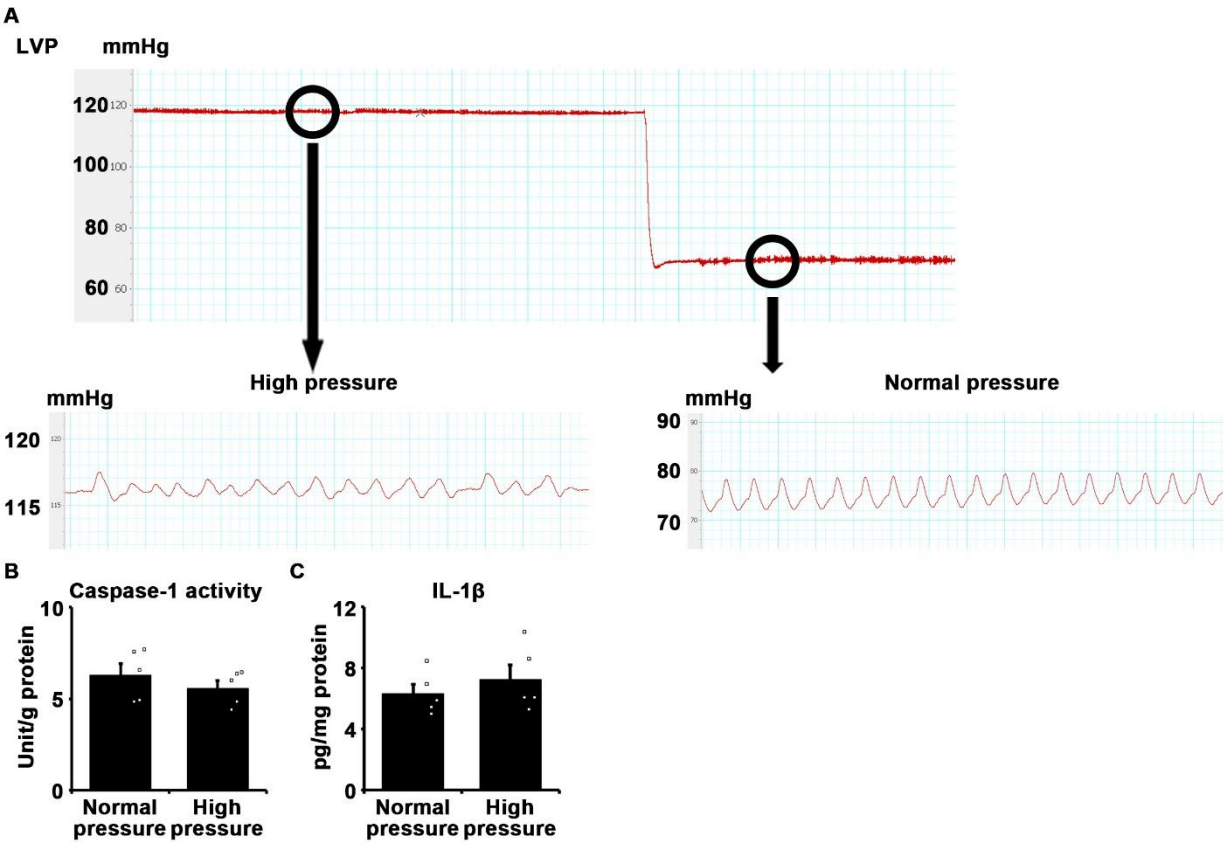

Supplemental Figure 16. NLRP3 Inflammasome Activity in Isolated Perfused Hearts *Ex Vivo*.

A, Left ventricle pressure (LVP) in isolated perfused murine heart. The Langendorff system was used for perfusion. LVP was measured using a mouse pressure-volume catheter. In our model, pressure overload of approximately 40 mmHg can be applied on murine hearts by increasing perfusion pressure. **B** and **C,** Myocardial caspase-1 activity (**B**) and IL-1β protein level (**C**) after 60 minutes of perfusion with normal or high pressure (n=5 per group). IL-1β protein was detected by ELISA. Values were normalized to total protein level. Differences in means between two groups were analyzed by unpaired two-tailed t-test. No significant differences in myocardial caspase-1 activity and IL-1β protein level were detected between isolated perfused murine hearts subjected to normal and high pressure. All error bars represent S.E.M.

SUPPLEMENTAL TABLE

Supplemental Table 1. Sequences of primers for quantitative RT-PCR.

Primer	Forward	Reverse	Product length
Mouse			
Nppa	GGGTAGGATTGACAGGATTGGA	CGACTGCCTTTTCCTCCTTG	91
Col1a1	CCGAACCCCAAGGAAAAGA	GTGGACATTAGGCGCAGGA	134
Vegfa	AAAAACGAAAGCGCAAGAAA	TTTCTCCGCTCTGAACAAGG	73
Tnfa	TCCCAGGTTCTCTTCAAGGGA	GGTGAGGAGCACGTAGTCGG	51
Il6	ACAACCACGGCCTTCCCTACTT	CACGATTTCCCAGAGAACATGTG	129
Mcp1	CCACTCACCTGCTGCTACTCAT	TGGTGATCCTCTTGTAGCTCTCC	76
Myh7	CAAGGTCAATACTCTGACCAAGG	CCATGCGCACTTTCTTCTC	95
Nlrp3	CCCTTGGAGACACAGGACTC	GAGGCTGCAGTTGTCTAATTCC	92
Asc	AGAGTACAGCCAGAACAGGACACTT	ATCCAGCACTCCGTCCACTT	86
Casp1	TCTGAAGAGGATTTCTTAACGGATG	GGTGTTGAAGAGCAGAAAGCAA	98
Il1β	TGAAGTTGACGGACCCCAAA	TGATGTGCTGCTGTGAGATT	101
Slc17a9	TGCTCTGGGCGTACTATGTG	AGGCCTTGAGCAAGGAATC	82
Nd6	AGGTGAAGGCTTTAATGCTAACCC	GGTCGCAGTTGAATGCTGTGT	103
Nd4	CATCACTCCTATTCTGCCTAGCAA	TCCTCGGGCCATGATTATAGTAC	74
Ndufa9	CCCGGGCCAGCTTACCT	GCTGCACTGCTTTCCTGATAGA	68
Cytb	GCCACCTTGACCCGATTCT	TTGCTAGGGCCGCGATAAT	64
Cytc	GGCTGCTGGATTCTCTTACACA	CCAAATACTCCATCAGGGTATCCT	80
Cox1	TTTTCAGGCTTCACCCTAGATGA	GAAGAATGTTATGTTTACTCCTACGAATAT	81
Cox2	CCATCCCAGGCCGACTAAA	TTTCAGAGCATTGGCCATAGAA	75
Cox3	CGGAAGTATTTTTCTTTGCAGGAT	CAGCAGCCTCCTAGATCATGTG	82
Cox4	TGCAGACCAAGCGAATGCT	TAGTCCCACTTGGCGGAGAA	67
Atp6	GGCTCCCGACACAAACTAAAAAG	TGGAATTAGTGAAATTGGAGTTCCT	72
Atp5f1a	ATGTGTCCGCTTACATTCCAACAA	GATCCGACACGGGACACAGA	130
Atp5f1b	ACATGGGCACAATGCAGGAA	GTCAGGTCATCAGCAGGCACA	91
Gapdh	ATGACAACTTTGTCAAGCTCATTT	GGTCCACCACCCTGTTGCT	69
Rat			
Nlrp3	GCTGTGTGAGGCACTCCAG	GAAACAGCATTGATGGGTCA	85
Gapdh	AGCTGGTCATCAATGGGAAA	ATTTGATGTTAGCGGGATCG	63
Human			
Nlrp3	AAAGAGATGAGCCGAAGTGG	GGTACTCCAGTAAACCCATCCA	108
Gapdh	CGCTCTCTGCTCCTCCTGTT	AAATCCGTTGACTCCGACCTT	110